

# ASYMPTOTICS OF UNIFORMLY RANDOM LOZENGE TILINGS OF POLYGONS. GAUSSIAN FREE FIELD<sup>1</sup>

BY LEONID PETROV

*Northeastern University and Institute for Information Transmission Problems*

We study large-scale height fluctuations of random stepped surfaces corresponding to uniformly random lozenge tilings of polygons on the triangular lattice. For a class of polygons (which allows arbitrarily large number of sides), we show that these fluctuations are asymptotically governed by a Gaussian free (massless) field. This complements the similar result obtained in Kenyon [*Comm. Math. Phys.* **281** (2008) 675–709] about tilings of regions without frozen facets of the limit shape.

In our asymptotic analysis we use the explicit double contour integral formula for the determinantal correlation kernel of the model obtained previously in Petrov [Asymptotics of random lozenge tilings via Gelfand–Tsetlin schemes (2012) Preprint].

**1. Introduction and main result.** We begin with a description of the model and formulation of necessary previous results which motivate the main result of the present paper. The latter is stated in Section 1.7 below.

1.1. *Model of uniformly random tilings.* Consider a polygon drawn on the regular triangular lattice as shown in Figure 1.

In the present paper we study the model of uniformly random tilings of such polygons by lozenges (= rhombi) of three types:



An example of such a tiling is presented in Figure 2, left. Equivalent formulations of the model include:

- (Dimer interpretation.) Lozenge tilings of a polygon are in a bijective correspondence with dimer coverings (= perfect matchings) on the part of the honeycomb graph located inside the polygon; see Figure 2, right.
- (Stepped surfaces.) One can view each tiling such as in Figure 2, left, as a 2-dimensional projection of a stepped surface, that is, of a continuous 3-

---

Received September 2012; revised November 2012.

<sup>1</sup>Supported in part by the RFBR-CNRS Grants 10-01-93114 and 11-01-93105.

*MSC2010 subject classifications.* Primary 60G55; secondary 60G15, 60C05, 82C22.

*Key words and phrases.* Random lozenge tilings, dimer model, height function, Gaussian free field, determinantal point processes.

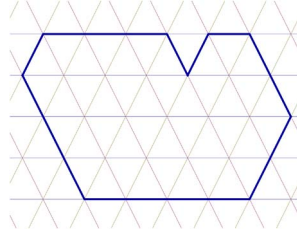


FIG. 1. Polygon on the triangular lattice.

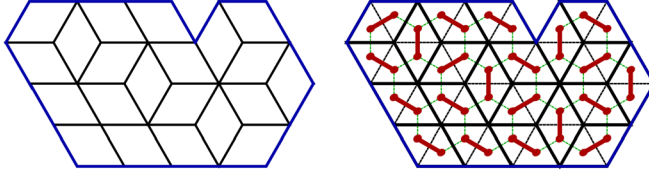


FIG. 2. Tiling of a polygon on the regular triangular lattice (left) and its dimer interpretation (right).

dimensional surface glued out of  $1 \times 1 \times 1$  boxes with sides parallel to three coordinate lines in space.

The model of uniformly random lozenge tilings of polygons has received significant attention over the past years: Cohn, Kenyon and Propp (2001), Kenyon and Okounkov (2007), Kenyon (2008). See also Kenyon (2009) for a detailed exposition of the subject and more references.

1.2. *Affine transform and the class of polygons.* For technical convenience, we perform a simple affine transform of lozenges which were present in Figure 2; see Figure 3. After this transform, tilings of polygons will look like the one in Figure 7 below. Polygons which are tiled will thus be drawn on the standard square grid, with all sides parallel either to one of the coordinate axes, or the vector  $(-1, 1)$ . We will denote the horizontal and the vertical integer coordinates on the square grid by  $x$  and  $n$ , respectively.

We will restrict ourselves to polygons of a special kind, as shown in Figure 4. Every polygon  $\mathbf{P}$  we consider can be parametrized by two integers  $N = 1, 2, \dots$ , and  $k = 2, 3, \dots$  (the polygon has  $3k$  sides), and by  $2k$  (proper) half-integers

$$A_1 < B_1 < A_2 < B_2 < \dots < A_k < B_k, \quad A_i, B_i \in \mathbb{Z}' := \mathbb{Z} + \frac{1}{2},$$

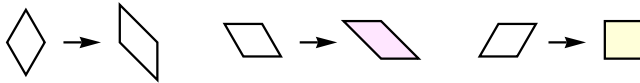


FIG. 3. Affine transform of lozenges.

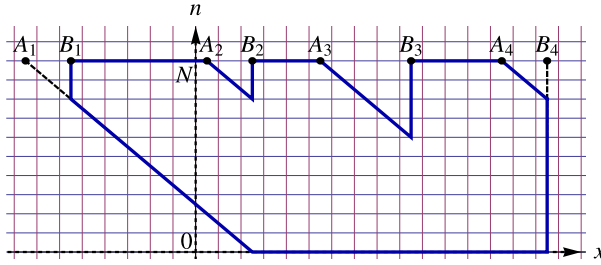


FIG. 4. A polygon from the class we consider. In this example  $k = 4$ , and the polygon has  $3k = 12$  sides.

subject to the condition  $\sum_{i=1}^k (B_i - A_i) = N$  which ensures that there is at least one lozenge tiling of  $\mathbf{P}$ . The bottom side of  $\mathbf{P}$  lies on the horizontal axis  $n = 0$ , and all the  $k - 1$  top sides [the  $i$ th such side has endpoints  $(B_i, N)$  and  $(A_{i+1}, N)$ ,  $i = 1, \dots, k - 1$ ] lie on one and the same line  $n = N$ .

1.3. *Height function of a tiling.* We will view our lozenge tilings (as on Figure 7 below) as projections of 3-dimensional stepped surfaces onto the  $(x, n)$  plane. The surface itself can thus be interpreted as a graph of a function  $h(x, n)$  which is called the *height function* of the tiling. To be concrete, let us stick to the convention that lozenges of type  $\sphericalangle$  correspond to horizontal planes, that is, planes where the height function is constant. We also require that  $h(x, n)$  is zero near the lower left corner of the polygon. See Figure 5 for an example and Section 3.1 below for a precise definition. See also [Kenyon (2009), Section 2.8] for more discussion.

The main object of the present paper is the height function corresponding to the uniformly random lozenge tiling of a polygon  $\mathbf{P}$ . We assume that  $\mathbf{P}$  belongs to the class of polygons described in Section 1.2. We denote this *random height function* by  $h_{\mathbf{P}}(x, n)$ .

1.4. *Limit shape.* We consider large  $N$  asymptotics of random tilings as all dimensions of the polygon  $\mathbf{P} = \mathbf{P}(N)$  grow. That is, let the parameters  $A_i(N)$ ,  $B_i(N)$

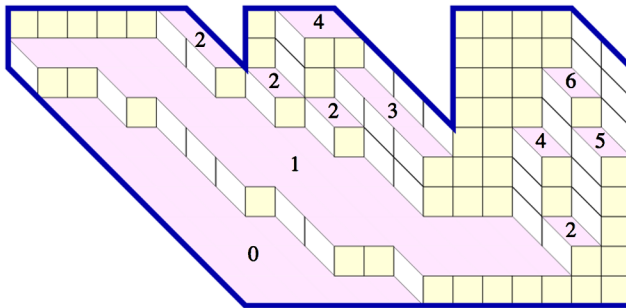


FIG. 5. Values of the height function  $h(x, n)$  on each horizontal plateau.

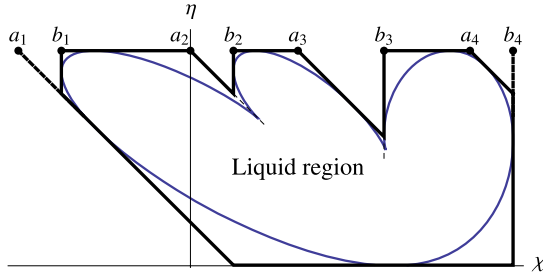


FIG. 6. The limiting polygon  $\mathcal{P}$  on the  $(\chi, \eta)$  plane and the frozen boundary curve.

of  $\mathbf{P}(N)$  behave as

$$(1) \quad A_i(N) = [a_i N] + \text{const}, \quad B_i(N) = [b_i N] + \text{const} \quad (i = 1, \dots, k).$$

Here  $a_1 < b_1 < \dots < a_k < b_k$  are new continuous parameters which satisfy  $\sum_{i=1}^k (b_i - a_i) = 1$ . The constants above are bounded uniformly in  $N$  and are needed to ensure that  $A_i(N), B_i(N) \in \mathbb{Z}'$  and  $\sum_{k=1}^N (B_i(N) - A_i(N)) = N$ .

In [Cohn, Kenyon and Propp \(2001\)](#) it was shown that in this  $N \rightarrow \infty$  regime, the rescaled random stepped surface concentrates around a nonrandom limit shape which can be obtained as a unique solution to a suitable variational problem; see also [Cohn, Larsen and Propp \(1998\)](#), [Destainville, Mosseri and Bailly \(1997\)](#) and [Destainville \(1998\)](#). This solution was described in [Kenyon and Okounkov \(2007\)](#) by means of the complex Burgers equation. For polygons we consider in the present paper, the limit shape is an algebraic surface.

More precisely, the limit shape result means that the height function  $h_{\mathbf{P}(N)}$  obeys the following law of large numbers (with almost sure convergence):

$$(2) \quad \frac{h_{\mathbf{P}(N)}([\chi N], [\eta N])}{N} \rightarrow \mathbf{h}(\chi, \eta), \quad N \rightarrow \infty,$$

where  $(\chi, \eta)$  are the new global continuous coordinates, and  $\mathbf{h}(\chi, \eta)$  is the function whose graph is the limit shape. The new coordinates  $(\chi, \eta)$  are assumed to belong to the limiting polygon  $\mathcal{P}$  which is parametrized by  $\{a_i, b_i\}_{i=1}^k$  in the same way as it was for  $\mathbf{P}(N)$  and  $\{A_i(N), B_i(N)\}_{i=1}^k$  in Section 1.2; see Figure 6. The new polygon  $\mathcal{P}$  is located inside the strip  $0 \leq \eta \leq 1$ .

A feature of the model we deal with is that the limit shape develops *frozen facets* where the function  $\mathbf{h}(\chi, \eta)$  is linear. In other words, frozen facets correspond to zones inside  $\mathcal{P}$  where lozenges of only one type are asymptotically present. Along with the frozen facets, there is a connected open *liquid region*  $\mathcal{D} \subset \mathcal{P}$ . For  $(\chi, \eta) \in \mathcal{D}$ , the limiting height function  $\mathbf{h}(\chi, \eta)$  is curved: asymptotically inside the liquid region one sees a random mixture of all types of lozenges; for example, see [Cohn, Larsen and Propp \[\(1998\), Figure 2\]](#), [Borodin and Gorin \[\(2009\), Figure 5\]](#), [Kenyon and Okounkov \[\(2007\), Figure 1\]](#) for illustrations of uniformly random tilings with small mesh where the limit shape and the frozen boundary are clearly seen.

REMARK 1.1. There are more precise results in this direction. Namely, the asymptotic local distribution of lozenges around a given global position  $(\chi, \eta) \in \mathcal{D}$  is governed by an ergodic translation invariant Gibbs measure on tilings of the whole plane. Such a measure is unique up to fixed proportions of lozenges of all types [Sheffield \(2005\)](#), and these proportions depend on the slope of the limit shape at the given point  $(\chi, \eta)$ . For polygons in the class described in Section 1.2, this result was established in [Petrov \(2012\)](#). For  $k = 2$  (when the polygon is a hexagon) this was obtained earlier in [Baik et al. \(2007\)](#), [Gorin \(2008\)](#). For tilings of regions when the limit shape has no frozen parts, the same local behavior was shown in [Kenyon \(2008\)](#). See also [Okounkov and Reshetikhin \(2003\)](#) and [Kenyon, Okounkov and Sheffield \(2006\)](#) for more detail on the limiting translation invariant ergodic Gibbs measures.

1.5. *Complex structure on the limit shape surface.* Complex coordinate on the limit shape surface was introduced in [Kenyon and Okounkov \(2007\)](#) [see also [Kenyon \(2008\)](#)], and by a different technique in [Petrov \(2012\)](#). From the results of [Petrov \(2012\)](#) it follows (see Section 4.2 below) that there exists a diffeomorphism  $w = w(\chi, \eta)$  from the liquid region  $\mathcal{D}$  to the upper half plane  $\mathbb{H} := \{z \in \mathbb{C} : \Im z > 0\}$ . [In [Petrov \(2012\)](#) the complex coordinate  $w$  was denoted by  $w_c$ .] The function  $w(\chi, \eta)$  is algebraic, and it satisfies the following degree  $k$  equation:

$$(3) \quad (w - \chi) \prod_{i=1}^k (w - a_i) = (w - \chi + 1 - \eta) \prod_{i=1}^k (w - b_i),$$

and a version of the differential complex Burgers equation [see also [Kenyon and Okounkov \(2007\)](#)],

$$(4) \quad \frac{w(\chi, \eta) - \chi}{1 - \eta} \cdot \frac{\partial w(\chi, \eta)}{\partial \chi} = - \frac{\partial w(\chi, \eta)}{\partial \eta}.$$

The complex coordinate  $w(\chi, \eta)$  can be used, in particular, to describe the local asymptotics of random tilings mentioned in Remark 1.1; see [Petrov \(2012\)](#), Sections 2.3–2.4 for more detail. The complex structure  $w(\chi, \eta)$  on the liquid region  $\mathcal{D}$  is employed in our description of asymptotics of fluctuations of the height function; see Section 1.7 below.

1.6. *Gaussian free field.* Before we proceed to describing our results, let us first briefly discuss the object which governs the asymptotics of fluctuations of the height function, namely, the Gaussian free field. This subsection is adapted from [Sheffield \(2007\)](#), see that survey for a detailed and systematic discussion.

The Gaussian free (massless) field GFF on the upper half plane  $\mathbb{H}$  is a probability Gaussian measure supported on a suitable class of generalized functions on  $\mathbb{H}$  (and not on ordinary functions). In particular, the value  $\text{GFF}(z)$  at a point  $z \in \mathbb{H}$  does not make sense.

The distribution of GFF may be understood as follows. For any sequence of compactly supported smooth test functions  $\{\phi_r\}_{r=1}^\infty$ , the pairings  $\{\text{GFF}(\phi_r)\}_{r=1}^\infty$  form a sequence of mean zero Gaussian random variables with covariances

$$\mathbb{E}(\text{GFF}(\phi_k)\text{GFF}(\phi_l)) = \int_{\mathbb{H} \times \mathbb{H}} |dz_1|^2 |dz_2|^2 \phi_k(z_1) \phi_l(z_2) \mathcal{G}(z_1, z_2).$$

Here  $(\cdot, \cdot)$  in the first integral is the usual inner product, and

$$(5) \quad \mathcal{G}(z, w) := -\frac{1}{2\pi} \ln \left| \frac{z-w}{z-\bar{w}} \right|, \quad z, w \in \mathbb{H}$$

is the Green function for the Laplace operator on the upper half plane  $\mathbb{H}$  with Dirichlet boundary conditions.

Even though the value of GFF at a point cannot be defined, one can still think that the expectations of products of values of GFF at pairwise distinct points  $z_1, \dots, z_s$  are well defined and are given by

$$\mathbb{E}(\text{GFF}(z_1) \cdots \text{GFF}(z_s)) = \begin{cases} \sum_{\sigma} \prod_{i=1}^{s/2} \mathcal{G}(z_{\sigma(2i-1)}, z_{\sigma(2i)}), & s \text{ even;} \\ 0, & s \text{ odd,} \end{cases}$$

with sum over all fixed point free involutions (= pairings)  $\sigma$  on  $\{1, \dots, s\}$ . Indeed, for a finite number of test functions,

$$(6) \quad \mathbb{E}(\text{GFF}(\phi_1) \cdots \text{GFF}(\phi_s)) = \int_{\mathbb{H}^s} \mathbb{E}(\text{GFF}(z_1) \cdots \text{GFF}(z_s)) \prod_{i=1}^s |dz_i|^2 \phi_i(z_i).$$

The moments (6) uniquely determine the Gaussian free field.

*1.7. Results.* Now we are in a position to describe the main results of the present paper. We are interested in asymptotics of fluctuations

$$(7) \quad H_N(\chi, \eta) := h_{\mathbf{P}(N)}([\chi N], [\eta N]) - \mathbb{E} h_{\mathbf{P}(N)}([\chi N], [\eta N])$$

of the height function (of a uniformly random tiling) around its mean.

**THEOREM 1.2 (Moment convergence of fluctuations to GFF).** *For pairwise distinct points  $(\chi_1, \eta_1), \dots, (\chi_s, \eta_s)$  inside the liquid region  $\mathcal{D}$ , as we scale the polygon  $\mathbf{P}(N)$  as in (1), the following convergence of moments holds:*

$$(8) \quad \begin{aligned} & \lim_{N \rightarrow \infty} \pi^{s/2} \mathbb{E}(H_N(\chi_1, \eta_1) \cdots H_N(\chi_s, \eta_s)) \\ &= \mathbb{E}(\text{GFF}(\mathbf{w}(\chi_1, \eta_1)) \cdots \text{GFF}(\mathbf{w}(\chi_s, \eta_s))) \\ &= \begin{cases} \sum_{\sigma} \prod_{i=1}^{s/2} \mathcal{G}(\mathbf{w}(\chi_{\sigma(2i-1)}, \eta_{\sigma(2i-1)}), \mathbf{w}(\chi_{\sigma(2i)}, \eta_{\sigma(2i)})), & s \text{ even;} \\ 0, & s \text{ odd,} \end{cases} \end{aligned}$$

where the sum is taken over all fixed point free involutions  $\sigma$  on  $\{1, \dots, s\}$ .

**THEOREM 1.3** (Central limit theorem for fluctuations of the height function). *The random function  $\sqrt{\pi} H_N(\chi, \eta)$  on  $\mathcal{D}$  weakly converges as  $N \rightarrow \infty$  to the w-pullback of the Gaussian free field GFF on  $\mathbb{H}$ .*

Theorem 1.3 means that for any smooth compactly supported test function  $\phi$  on  $\mathcal{D}$ , we have the weak convergence as  $N \rightarrow \infty$ ,

$$(9) \quad \begin{aligned} \sqrt{\pi} \int_{\mathcal{D}} \phi(\chi, \eta) H_N(\chi, \eta) d\chi d\eta &\rightarrow \int_{\mathcal{D}} \phi(\chi, \eta) \text{GFF}(w(\chi, \eta)) d\chi d\eta \\ &= \int_{\mathbb{H}} \phi(w^{-1}(z)) J(z) \text{GFF}(z) |dz|^2, \end{aligned}$$

where  $J(z)$  is the Jacobian of the change of variables  $z \rightarrow (\chi, \eta)$  by  $w^{-1}$  [which in fact can be explicitly calculated using (3)–(4)]. Theorem 1.3 follows from Theorem 1.2 plus an additional bound on moments of fluctuations of the height function at infinitesimally close points; see Section 5.4.

It is worth noting that Gaussian free field fluctuations in random tiling models were also obtained [along with Kenyon (2008)] in Borodin and Ferrari (2008), Duits (2011) and Kuan (2011).

**1.8. Strategy of the proof and organization of the paper.** Our proof is based on an explicit formula for the determinantal correlation kernel of uniformly random tilings which was established in Petrov (2012). We recall these results in Section 2. In Section 3 we write the multipoint fluctuations  $\mathbb{E}(H_N(\chi_1, \eta_1) \cdots H_N(\chi_s, \eta_s))$  of the height function in terms of that correlation kernel. This allows us to establish Theorem 1.2 and then Theorem 1.3 in Section 5 using certain fine asymptotic properties of the correlation kernel which are obtained in Section 4.

Our argument generally follows the approach of Borodin and Ferrari (2008) (especially see Section 5 in that paper) which in turn was partly inspired by Kenyon (2008). We also use some ideas from Duits (2011). However, our correlation kernel has a more complicated structure than those of Borodin and Ferrari (2008) and Duits (2011): the critical points of the action (Section 4.2) which are solutions of (3) cannot be determined explicitly. Thus, in our Section 4 in order to investigate asymptotics of the kernel, we must employ certain new considerations (Sections 4.3–4.4).

**2. Determinantal structure of random tilings.** In this section we recall the formula of Petrov (2012) for the determinantal correlation kernel of our model of uniformly random tilings. Then we extend that kernel and describe the joint distribution of all three types of lozenges in our random tiling. Except for Section 2.4, this section is essentially taken from Petrov (2012).

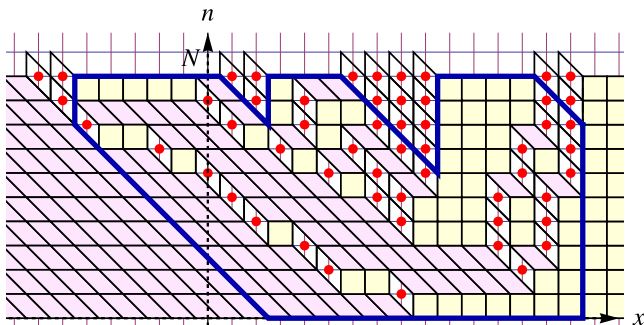


FIG. 7. Tiling of a polygon and the corresponding interlacing particle array.

2.1. *Interlacing particle arrays.* Let  $\mathbf{P}$  be a polygon of our class in the  $(x, n)$  plane (see Section 1.2) contained inside the horizontal strip  $0 \leq n \leq N$ . We pass from tilings of  $\mathbf{P}$  to interlacing particle arrays as follows. We first trivially extend any tiling of  $\mathbf{P}$  to a tiling of the whole strip  $0 \leq n \leq N$  with  $N$  small triangles added on top; see Figure 7. Then we place a particle in the center of every lozenge of type  $\searrow$ .

Thus, we get a particle array  $\mathbf{X} := \{\mathbf{x}_j^m : m = 1, \dots, N; j = 1, \dots, m\} \in \mathbb{Z}^{N(N+1)/2}$  with precisely  $m$  particles at each  $m$ th horizontal level,  $m = 0, 1, \dots, N$ . Because we started from a tiling of  $\mathbf{P}$ , these particles must satisfy the *interlacing constraints*

$$(10) \quad \mathbf{x}_{j+1}^m < \mathbf{x}_j^{m-1} \leq \mathbf{x}_j^m$$

(for all  $j$ 's and  $m$ 's for which these inequalities can be written out). Moreover, the particles in the top row of the array are fixed,

$$(11) \quad \begin{aligned} & \{\mathbf{x}_N^N < \dots < \mathbf{x}_1^N\} \\ & = \{A_1 + \frac{1}{2} < A_1 + \frac{3}{2} < \dots < B_1 - \frac{3}{2} < B_1 - \frac{1}{2} \\ & \quad < A_2 + \frac{1}{2} < \dots < B_2 - \frac{1}{2} < \dots < A_k + \frac{1}{2} < \dots < B_k - \frac{1}{2}\} \end{aligned}$$

(here  $\{A_i, B_i\}_{i=1}^k$  are the parameters of  $\mathbf{P}$ ; see Section 1.2). Clearly, lozenge tilings of  $\mathbf{P}$  and such interlacing arrays  $\mathbf{X}$  with fixed top row (11) are in a bijective correspondence. For a connection of these arrays with Gelfand–Tsetlin schemes (an object related to branching of representations of unitary groups), see, for example, Petrov (2012), Section 3.

2.2. *Determinantal correlation kernel.* We see from Section 2.1 that the uniform measure on the set of all tilings of the polygon  $\mathbf{P}$  is the same as the uniform measure on the space of interlacing integer arrays  $\mathbf{X} = \{\mathbf{x}_j^m\}$  with fixed top row (11).



We denote both measures by  $\mathbb{P}_{\mathbf{P}}$ . Viewing  $X$  as a particle configuration, we can also think of the measure  $\mathbb{P}_{\mathbf{P}}$  as of a point process on  $\mathbb{Z} \times \{1, 2, \dots, N\}$ .

**DEFINITION 2.1.** Let  $(x_1, n_1), \dots, (x_s, n_s)$  be pairwise distinct positions,  $x_i \in \mathbb{Z}$ ,  $1 \leq n_i \leq N$ . The *correlation functions* of the point process  $\mathbb{P}_{\mathbf{P}}$  are defined as

$$\rho_{\mathbf{s}}(x_1, n_1; \dots; x_s, n_s) := \mathbb{P}_{\mathbf{P}}(\text{there is a particle of the random configuration } \{x_j^m\} \text{ at position } (x_i, n_i) \text{ for every } i = 1, \dots, s).$$

It is well known that the measure  $\mathbb{P}_{\mathbf{P}}$  on interlacing particle arrays is *determinantal* (for instance, this fact can be deduced from the Kasteleyn theory; see Section 2.3 below). That is, there exists a function  $K(x, n; y, m)$  (the *correlation kernel*), such that

$$(12) \quad \rho_{\mathbf{s}}(x_1, n_1; \dots; x_s, n_s) = \det[K(x_i, n_i; x_j, n_j)]_{i,j=1}^s$$

for any  $\mathbf{s}$  and any collection of pairwise distinct positions  $(x_1, n_1), \dots, (x_s, n_s)$ . About determinantal point processes in general see the surveys [Soshnikov \(2000\)](#), [Hough et al. \(2006\)](#), [Borodin \(2011\)](#).

In [Petrov \(2012\)](#) the following explicit formula for the correlation kernel  $K$  of random interlacing arrays  $X$  with fixed top row (11) was obtained:

**THEOREM 2.2 [[Petrov \(2012\)](#)].** For  $1 \leq n_1 \leq N$ ,  $1 \leq n_2 \leq N - 1$  and  $x_1, x_2 \in \mathbb{Z}$ , the correlation kernel of the point process  $\mathbb{P}_{\mathbf{P}}$  has the form<sup>2</sup>

$$(13) \quad \begin{aligned} & K(x_1, n_1; x_2, n_2) \\ &= -1_{n_2 < n_1} 1_{x_2 \leq x_1} \frac{(x_1 - x_2 + 1)_{n_1 - n_2 - 1}}{(n_1 - n_2 - 1)!} + \frac{(N - n_1)!}{(N - n_2 - 1)!} \\ & \times \frac{1}{(2\pi i)^2} \oint_{\mathcal{C}(x_2)} dz \oint_{\mathcal{C}(\infty)} dw \frac{(z - x_2 + 1)_{N - n_2 - 1}}{(w - x_1)_{N - n_1 + 1}} \frac{1}{w - z} \\ & \times \prod_{i=1}^k \frac{(A_i + 1/2 - w)_{B_i - A_i}}{(A_i + 1/2 - z)_{B_i - A_i}}. \end{aligned}$$

The contours in  $z$  and  $w$  are positively (counter-clockwise) oriented and do not intersect. The contour  $\mathcal{C}(x_2)$  in  $z$  encircles the integer points  $x_2, x_2 + 1, \dots, B_k - \frac{1}{2}$  and only them (i.e., does not contain  $x_2 - 1, x_2 - 2, \dots$  and  $B_k + \frac{1}{2}, B_k + \frac{3}{2}, \dots$ ). The contour  $\mathcal{C}(\infty)$  in  $w$  contains  $\mathcal{C}(x_2)$  and all the points  $x_1, x_1 - 1, \dots, x_1 - (N - n_1)$ .

The above explicit formula for the kernel  $K$  is our main tool in the present paper.

<sup>2</sup>Here and below  $1_{\{\dots\}}$  denotes the indicator of a set, and  $(y)_m := y(y + 1) \cdots (y + m - 1)$ ,  $m = 1, 2, \dots$  [with  $(y)_0 := 1$ ] is the Pochhammer symbol.

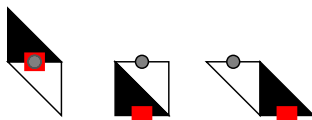


FIG. 8. Edges of three directions in the graph  $G_{\mathbf{P}}$  encoded by pairs of triangles.

2.3. *Inverse Kasteleyn matrix.* Here let us recall the connection [Petrov (2012), Section 6] between the above kernel  $K$  (Theorem 2.2) and the Kasteleyn matrix of the honeycomb graph  $G_{\mathbf{P}}$  inside our polygon  $\mathbf{P}$  (Figure 2, right). We will use it to write down the joint distribution of three types of lozenges  $\blacktriangledown$ ,  $\square$  and  $\blacktriangleleft$  in Section 2.4 below.

The honeycomb graph  $G_{\mathbf{P}}$  is bipartite; its vertices correspond to two types of (triangle) faces in the dual triangular lattice,



We will encode each such triangle by the position  $(x, n)$  of the mid-point of its horizontal side. The Kasteleyn matrix of the graph  $G_{\mathbf{P}}$  is its adjacency matrix with rows and columns parametrized by white and black triangles, respectively; for example, see Kenyon (2009). Inside the polygon, this matrix looks as

$$(14) \quad \text{Kast}(\blacktriangledown(x, n); \blacktriangleleft(y, m)) = \begin{cases} 1, & \text{if } (y, m) = (x, n); \\ 1, & \text{if } (y, m) = (x, n - 1); \\ 1, & \text{if } (y, m) = (x + 1, n - 1); \\ 0, & \text{otherwise;} \end{cases}$$

see Figure 8. For  $\blacktriangledown(x, n)$  on the boundary of the graph  $G_{\mathbf{P}}$ , the  $\blacktriangledown(x, n)$ th row of  $\text{Kast}$  will contain less than three ones, and the same for the  $\blacktriangleleft(y, m)$ th column.

It is known that the determinant  $\det[\text{Kast}(\blacktriangledown(x, n); \blacktriangleleft(y, m))]$ , where  $\blacktriangledown(x, n)$  and  $\blacktriangleleft(y, m)$  run over all possible white and black triangles in  $G_{\mathbf{P}}$ , is equal to the total number of lozenge tilings of the polygon  $\mathbf{P}$ . As [Kenyon (2009), Corollary 3] suggests,  $\text{Kast}^{-1}$  can serve as a correlation kernel for the uniform measure on tilings of  $\mathbf{P}$ . A more precise statement is as follows:

**THEOREM 2.3** [Petrov (2012)]. *The inverse Kasteleyn matrix and the correlation kernel  $K$  of Theorem 2.2 are related as follows [for all possible values of  $(x, n)$  and  $(y, m)$ ]:*

$$\text{Kast}^{-1}(\blacktriangleleft(y, m); \blacktriangledown(x, n)) = (-1)^{y-x+m-n} K(x, n; y, m).$$

2.4. *Extension of  $K$  and joint distribution of three types of lozenges.* Here we compute probabilities that a random tiling has lozenges of prescribed types at prescribed positions (i.e., the joint distribution of all types of lozenges). These probabilities are given by determinants similar to the correlation functions of interlacing particle arrays (Definition 2.1), but with an extended kernel.

Let, by agreement, the position of every lozenge be encoded by the position of its white triangle (i.e., by the position of the circle dot on Figure 8). We introduce the following extended kernel (here and below  $\theta_j \in \{\blacktriangleright, \square, \blacktriangleright\}$  are types of lozenges):

$$(15) \quad K_\theta(x_1, n_1, \theta_1; x_2, n_2, \theta_2) := \begin{cases} K(x_1, n_1; x_2, n_2), & \text{if } \theta_2 = \blacktriangleright; \\ -K(x_1, n_1; x_2, n_2 - 1), & \text{if } \theta_2 = \square; \\ K(x_1, n_1; x_2 + 1, n_2 - 1), & \text{if } \theta_2 = \blacktriangleright. \end{cases}$$

PROPOSITION 2.4. *For any collection of lozenges of types  $\theta_1, \dots, \theta_s \in \{\blacktriangleright, \square, \blacktriangleright\}$  at (pairwise distinct) positions  $(x_i, n_i)$ ,  $i = 1, \dots, s$ , we have*

$$\begin{aligned} & \mathbb{P}_{\mathbf{P}}(\text{There is a lozenge of type } \theta_r \text{ at } (x_r, n_r) \text{ for all } r = 1, \dots, s) \\ &= \det[K_\theta(x_i, n_i, \theta_i; x_j, n_j, \theta_j)]_{i,j=1}^s. \end{aligned}$$

PROOF. This is a direct consequence of the above Theorem 2.3 and also of Kenyon (2009), Corollary 3. Namely:

- there is a lozenge of type  $\blacktriangleright$  at  $(x, n)$  if and only if the dimer covering contains the edge  $(\blacktriangle(x, n); \blacktriangleright(x, n))$ ;
- there is a lozenge of type  $\square$  at  $(x, n)$  if and only if the dimer covering contains the edge  $(\blacktriangle(x, n - 1); \blacktriangleright(x, n))$ ;
- there is a lozenge of type  $\blacktriangleright$  at  $(x, n)$  if and only if the dimer covering contains the edge  $(\blacktriangle(x + 1, n - 1); \blacktriangleright(x, n))$ .

Then, using Kenyon (2009), Corollary 3, we can write the probability

$$\mathbb{P}_{\mathbf{P}}(\text{There is a lozenge of type } \theta_r \text{ at } (x_r, n_r) \text{ for all } r = 1, \dots, s)$$

as a determinant of a suitable matrix with entries  $\text{Kast}^{-1}$ . In this matrix there will be three types of rows (recall that they are indexed by black triangles) corresponding to different types of lozenges as above. Then, using the relation between  $\text{Kast}^{-1}$  and the kernel  $K$  (Theorem 2.3), we complete the proof.  $\square$

A similar property for a different tiling model (of an infinite region) was obtained in Borodin and Ferrari (2008), Theorem 5.2; see also Borodin, Gorin and Rains (2010), Section 7.2.

**3. Height function and its multipoint fluctuations.** In this section we discuss the concept of a height function of a tiling. In Section 3.3, for our model of uniformly random tilings, we express the multipoint moments of fluctuations of the height function through the correlation kernel  $K$  of Theorem 2.2.

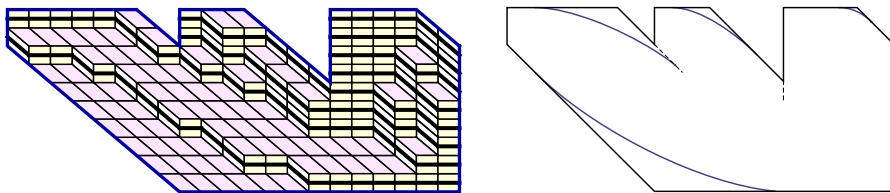


FIG. 9. “Level lines” of the height function (left) and the corresponding parts of the frozen boundary (right).

3.1. *Definition of the height function.* Let  $\mathbf{P}$  be a polygon from our class (Section 1.2). Fix a tiling of  $\mathbf{P}$ . It is possible to define the *height function* of this tiling which at every position  $(x, n) \in \mathbf{P}$  is equal to

$$(16) \quad h(x, n) := \sum_{m: m \leq n} 1_{\{\text{there is a lozenge of type } \heartsuit \text{ or } \square \text{ at } (x, m)\}}.$$

Clearly, this implies that the height function is constant on each horizontal plateau consisting of lozenges of type  $\heartsuit$ ; see Figure 5.

With every tiling one can associate three families of nonintersecting lattice paths; for example, see Petrov (2012), Section 2.5. Nonintersecting paths in one of these families shown in Figure 9 (left) can serve as “level lines” of the height function. Namely,  $h(x, n)$  at a given point is equal to the number of these nonintersecting paths lying between  $(x, n)$  and the line  $n = 0$ . See also Figure 7 where the tiling is extended so that formula (16) and the interpretation with the “level lines” make full sense.

REMARK 3.1. The two other families of nonintersecting paths [Petrov (2012), Section 2.5] give two other possible ways to define the height function; see also Kenyon (2009), Section 2.8 for a more detailed discussion.

3.2. *Paths to the boundary.* Now let  $\mathbf{P}(N)$  be a sequence of polygons scaled as explained in Section 1.4. We would like to study asymptotics of multipoint fluctuations of the random height function  $h_{\mathbf{P}(N)}$  [corresponding to the uniformly random tiling of  $\mathbf{P}(N)$ ] around global positions  $(\chi_1, \eta_1), \dots, (\chi_s, \eta_s) \in \mathcal{D}$ . Here  $\mathcal{D}$  is the liquid region (Figure 6). Namely, we are interested in the asymptotic behavior of the expectations entering (8),

$$(17) \quad \mathbb{E}(H_N(\chi_1, \eta_1) \cdots H_N(\chi_s, \eta_s)),$$

where  $H_N(\chi_j, \eta_j)$ 's are the fluctuations of the height function defined in (7).

To compute values of the height function entering (17), one could use formula (16). But then several indicators corresponding to the same point  $(x, m)$  in (16) will enter the resulting expression. This will lead to certain technical complications which we can easily avoid. Namely, let us choose  $s$  piecewise-linear

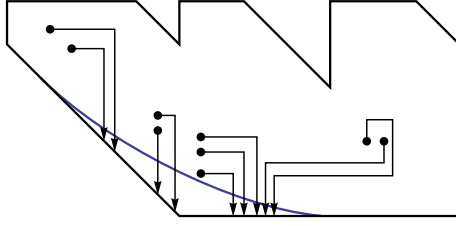


FIG. 10. Paths to the frozen boundary along which we calculate the height function at  $([\chi_i N], [\eta_i N])$ ,  $i = 1, \dots, s$ .

simple paths with horizontal and vertical pieces such that each  $i$ th path connects  $([\chi_i N], [\eta_i N])$  and the lower left part of the frozen boundary as in Figure 10. We choose this part of  $\partial\mathcal{D}$  because on the corresponding facet the height function will be asymptotically equal to zero; cf. Figure 5. By agreement, we assume that while crossing the frozen boundary, each path goes in a vertical direction and proceeds vertically down until it hits the boundary of the polygon. By taking  $N$  larger if necessary, we require that these  $s$  paths do not intersect.<sup>3</sup> We also require the number of piecewise-linear segments in each path to be bounded (uniformly in  $N$ ).

Such paths can be constructed using the diffeomorphism  $w: \mathcal{D} \rightarrow \mathbb{H}$  (see Section 1.5 and Section 4.2 below) which maps the frozen boundary to the real line. It is not hard to show that in  $\mathbb{H}$  the desired (continuous) nonintersecting paths exist. Then in  $\mathcal{D}$  we can approximate the images of these paths under  $w^{-1}$  by piecewise-linear paths. Since the number of points  $(\chi_i, \eta_i)$  (and paths) is finite, we can also make sure that the number of segments in these paths is bounded uniformly in  $N$ .

REMARK 3.2. We could also use paths ending at any part of the frozen boundary in Figure 9 (right) because on the corresponding facets our height function asymptotically becomes constant, and we subtract this constant in the definition of  $H_N$  (7). However, we use only paths as in Figure 10 to simplify the notation in Section 4.6 below.

DEFINITION 3.3. For integers  $x < x'$  and  $n$ , denote

$$(18) \quad H_{x,x'}(n) := \sum_{y=x+1}^{x'} 1\{\text{there is a lozenge of type } \blacktriangleright \text{ at } (y, n)\}.$$

Also, for integers  $n < n'$  and  $y$ , set

$$(19) \quad V_{n,n'}(y) := \sum_{m=n+1}^{n'} 1\{\text{there is a lozenge of type } \blacktriangleright \text{ or } \square \text{ at } (y, m)\}.$$

<sup>3</sup>Except for the case when some of the points  $(\chi_i, \eta_i)$  coincide; then we still do not allow intersections away from the starting points  $([\chi_i N], [\eta_i N])$ .

Above we have explained how each individual fluctuation  $H_N(\chi_i, \eta_i)$ ,  $i = 1, \dots, s$ , can be written as a finite linear combination (with coefficients  $\pm 1$ ) of expressions of the form  $H_{x_i, x'_i}(n_i) - \mathbb{E}H_{x_i, x'_i}(n_i)$  and  $V_{n_j, n'_j}(x_j) - \mathbb{E}V_{n_j, n'_j}(x_j)$ .<sup>4</sup> Moreover, if all the points  $(\chi_i, \eta_i)$  are distinct, then each indicator entering any of the sums (18) and (19) corresponding to  $(\chi_i, \eta_i)$ ,  $i = 1, \dots, s$ , appears only once because our paths to the boundary do not intersect.

**3.3. Expectation of a product of horizontal and vertical sums.** Let all the points  $(\chi_i, \eta_i)$ ,  $i = 1, \dots, s$ , be distinct. From the discussion of Section 3.2, it follows that our expectation (17) can be expressed as a linear combination (with coefficients  $\pm 1$ ) of terms of the form

$$(20) \quad \mathbb{E} \left( \prod_{i=1}^r (H_{x_i, x'_i}(n_i) - \mathbb{E}H_{x_i, x'_i}(n_i)) \prod_{j=r+1}^s (V_{n_j, n'_j}(x_j) - \mathbb{E}V_{n_j, n'_j}(x_j)) \right)$$

such that the following horizontal and vertical segments,

$$\begin{aligned} \{(y, n_i) : y = x_i + 1, \dots, x'_i\}, & \quad i = 1, \dots, r; \\ \{(x_j, m) : m = n_j + 1, \dots, n'_j\}, & \quad j = r + 1, \dots, s, \end{aligned}$$

do not intersect. Here and below we assume that  $x_i < x'_i$ ,  $n_j < n'_j$  for all  $i, j$ .

**PROPOSITION 3.4** [cf. Borodin and Ferrari (2008), Lemma 5.3]. *With the above notation and assumptions, expression (20) can be written in the following form:*

$$(21) \quad \sum_{y_1=x_1+1}^{x'_1} \cdots \sum_{y_r=x_r+1}^{x'_r} \sum_{m_{r+1}=n_{r+1}+1}^{n'_{r+1}} \cdots \sum_{m_s=n_s+1}^{n'_s} \det \begin{bmatrix} A_{1,1} & A_{1,2} \\ A_{2,1} & A_{2,2} \end{bmatrix}.$$

The matrix blocks are given by

$$(22) \quad \begin{aligned} A_{1,1} &= [(1 - \delta_{ij})K(y_i, n_i; y_j, n_j)]_{i,j=1,\dots,r}, \\ A_{1,2} &= [K(y_i, n_i; x_j + 1, m_j - 1)]_{i=1,\dots,r; j=r+1,\dots,s}, \\ A_{2,1} &= [-K(x_i, m_i; y_j, n_j)]_{i=r+1,\dots,s; j=1,\dots,r}, \\ A_{2,2} &= [-(1 - \delta_{ij})K(x_i, m_i; x_j + 1, m_j - 1)]_{i,j=r+1,\dots,s}. \end{aligned}$$

**PROOF.** As was observed in [Kenyon (2008), Proof of Theorem 7.2], the subtraction of the means in (20) leads to vanishing of the diagonal matrix elements in  $A_{1,1}$  and  $A_{2,2}$  in (22). Thus, it suffices to consider  $\mathbb{E}(\prod_{i=1}^r H_{x_i, x'_i}(n_i) \times \prod_{j=r+1}^s V_{n_j, n'_j}(x_j))$ . We write every  $H_{x_i, x'_i}(n_i)$  and  $V_{n_j, n'_j}(x_j)$  as the corresponding

<sup>4</sup>Note that the height function vanishes at the end of each path in Figure 10.

sum (18)–(19). After taking the expectation, we get an  $s$ -fold sum as in (21) with terms

$$\begin{aligned}
 & \mathbb{P}_{\mathbf{P}(N)}(\text{There is a lozenge of type } \heartsuit \text{ at } (y_i, n_i), i = 1, \dots, r; \\
 & \quad \text{and of type } \heartsuit \text{ or } \square \text{ at } (x_j, m_j), j = r + 1, \dots, \mathbf{s}) \\
 (23) \quad & = \mathbb{P}_{\mathbf{P}(N)}(\text{There is a lozenge of type } \heartsuit \text{ at } (y_i, n_i), i = 1, \dots, r; \\
 & \quad \text{and there is no lozenge of type } \heartsuit \text{ at } (x_j, m_j), j = r + 1, \dots, \mathbf{s}).
 \end{aligned}$$

The latter probability can be expressed as an  $s \times s$  determinant which has the structure

$$\det \left[ \begin{array}{c} K_{\theta}^{\Delta}(y_i, n_i, \heartsuit; y_{i'}, n_{i'}, \heartsuit) \\ K_{\theta}^{\Delta}(x_j, m_j, \heartsuit; y_{i'}, n_{i'}, \heartsuit) \\ K_{\theta}^{\Delta}(y_i, n_i, \heartsuit; x_{j'}, m_{j'}, \heartsuit) \\ K_{\theta}^{\Delta}(x_j, m_j, \heartsuit; x_{j'}, m_{j'}, \heartsuit) \end{array} \right]_{i, i' = 1, \dots, r; j, j' = r + 1, \dots, \mathbf{s}}.$$

Here  $K_{\theta}^{\Delta}$  is the kernel which is obtained from  $K_{\theta}$  (15) via a particle-hole involution [e.g., see Borodin, Okounkov and Olshanski (2000), Appendix A.3] at positions  $\{(x_j, m_j)\}_{j=r+1}^{\mathbf{s}}$ . That kernel  $K_{\theta}^{\Delta}$  looks as follows (see also Proposition 2.4):

$$\begin{aligned}
 K_{\theta}^{\Delta}(y_i, n_i, \heartsuit; y_{i'}, n_{i'}, \heartsuit) &= K(y_i, n_i; y_{i'}, n_{i'}); \\
 K_{\theta}^{\Delta}(y_i, n_i, \heartsuit; x_{j'}, m_{j'}, \heartsuit) &= K_{\theta}(y_i, n_i, \heartsuit; x_{j'}, m_{j'}, \heartsuit) \\
 &= K(y_i, n_i; x_{j'} + 1, m_{j'} - 1); \\
 K_{\theta}^{\Delta}(x_j, m_j, \heartsuit; y_{i'}, n_{i'}, \heartsuit) &= -K_{\theta}(x_j, m_j, \heartsuit; y_{i'}, n_{i'}, \heartsuit) \\
 &= -K(x_j, m_j; y_{i'}, n_{i'}); \\
 K_{\theta}^{\Delta}(x_j, m_j, \heartsuit; x_{j'}, m_{j'}, \heartsuit) &= \delta_{j, j'} - K_{\theta}(x_j, m_j, \heartsuit; x_{j'}, m_{j'}, \heartsuit) \\
 &= \delta_{j, j'} - K(x_j, m_j; x_{j'} + 1, m_{j'} - 1).
 \end{aligned}$$

Then, setting the diagonal matrix elements to zero, we obtain matrix blocks (22). This completes the proof.  $\square$

**REMARK 3.5.** Representation of Proposition 3.4 is not valid if some of the points  $(\chi_j, \eta_j)$  coincide because then we cannot write all the probabilities (23) as  $s \times s$  determinants. In this case, in the asymptotic analysis of multipoint fluctuations (17) we employ Lemma 5.6 below.

**4. Asymptotics of the kernel.** In this section we investigate asymptotic properties of the correlation kernel of Theorem 2.2 in various regimes.

4.1. *Action*  $S(w; \chi, \eta)$ . The polygon  $\mathbf{P}(N)$  is assumed to be scaled as in Section 1.4. We will be interested in asymptotics of the kernel  $K(x_1, n_1; x_2, n_2)$  when the two points  $(x_1, n_1)$  and  $(x_2, n_2)$  behave as

$$(24) \quad \frac{x_j}{N} \rightarrow \chi_j, \quad \frac{n_j}{N} \rightarrow \eta_j, \quad j = 1, 2,$$

where  $(\chi_1, \eta_1)$  and  $(\chi_2, \eta_2)$  are two (not necessarily distinct) global positions inside the limiting polygon  $\mathcal{P}$ ; see Section 1.4 and especially Figure 6.

DEFINITION 4.1 [Petrov (2012), Section 7.2]. Define the *action* by

$$(25) \quad \begin{aligned} & S(w; \chi, \eta) \\ & := (w - \chi) \ln(w - \chi) - (w - \chi + 1 - \eta) \ln(w - \chi + 1 - \eta) \\ & \quad + (1 - \eta) \ln(1 - \eta) + \sum_{i=1}^k [(b_i - w) \ln(b_i - w) - (a_i - w) \ln(a_i - w)]. \end{aligned}$$

Unless otherwise stated, we assume that the branches of all logarithms have cuts looking in negative direction along the real line. Note that the real part  $\Re S(w; \chi, \eta)$  is well defined and continuous for all  $w \in \mathbb{C}$ .

Denote also

$$\Xi(w; \chi, \eta) := \frac{(w - \chi)(w - \chi + 1 - \eta)}{1 - \eta}$$

and

$$(26) \quad \Xi_j(w) := \Xi\left(w; \frac{x_j}{N}, \frac{n_j}{N}\right), \quad S_j(w) := S\left(w; \frac{x_j}{N}, \frac{n_j}{N}\right), \quad j = 1, 2.$$

PROPOSITION 4.2. *In regime (24), the kernel  $K(x_1, n_1; x_2, n_2)$  of Theorem 2.2 has the following asymptotics:*

$$(27) \quad \begin{aligned} & K(x_1, n_1; x_2, n_2) \\ & = -1_{n_2 < n_1} \left(1 + O\left(\frac{1}{N}\right)\right) \frac{1}{2\pi i} \oint_{\mathfrak{C}(\chi_2-)} \frac{\exp\{N(S_1(z) - S_2(z))\}}{\sqrt{\Xi_1(z)\Xi_2(z)}} dz \\ & \quad + \left(1 + O\left(\frac{1}{N}\right)\right) \\ & \quad \times \frac{1}{(2\pi i)^2} \oint_{\mathfrak{C}(\chi_2-)} dz \oint_{\mathfrak{C}(\infty)} dw \frac{1}{w - z} \frac{\exp\{N(S_1(w) - S_2(z))\}}{\sqrt{\Xi_1(w)\Xi_2(z)}}. \end{aligned}$$

Here  $z$  in both single and double integrals runs over a counter-clockwise contour which crosses the real line just to the left of  $\chi_2$ , and also to the right of  $b_k \sim \frac{B_K}{N}$ ; see (1). The  $w$  contour is counter-clockwise, contains  $\mathfrak{C}(\chi_2-)$  (without intersecting it) and is sufficiently large.



When  $(\chi_1, \eta_1) = (\chi_2, \eta_2)$ , this essentially coincides with [Petrov \(2012\)](#), Proposition 7.2.

**PROOF OF PROPOSITION 4.2.** Let us adapt the double contour integral in formula (13) to the asymptotic regime (24) by scaling the variables as  $\tilde{z} = z/N$ ,  $\tilde{w} = w/N$  (and then renaming back to  $z, w$ ),

$$\begin{aligned} K(x_1, n_1; x_2, n_2) &= -1_{n_2 < n_1} 1_{x_2 \leq x_1} \frac{(x_1 - x_2 + 1)_{n_1 - n_2 - 1}}{(n_1 - n_2 - 1)!} + \frac{N(N - n_1)!}{(N - n_2 - 1)!} \\ &\quad \times \frac{1}{(2\pi i)^2} \oint_{\mathcal{C}(\chi_2^-)} dz \oint_{\mathcal{C}(\infty)} dw \frac{(Nz - x_2 + 1)_{N - n_2 - 1}}{(Nw - x_1)_{N - n_1 + 1}} \frac{1}{w - z} \\ &\quad \times \prod_{i=1}^k \frac{(A_i + 1/2 - Nw)_{B_i - A_i}}{(A_i + 1/2 - Nz)_{B_i - A_i}}. \end{aligned}$$

Here  $z$  and  $w$  run over the corresponding scaled contours, and they can be chosen independently of  $N$ .<sup>5</sup> These contours coincide with the ones in the claim (27).

Expressing all the Pochhammer symbols in the integrand above through the Gamma function and applying the Stirling approximation, we may write for non-real  $z, w$  [see [Petrov \(2012\)](#), Section 7.2 for more detail],

$$\begin{aligned} &\frac{1}{w - z} \frac{N(N - n_1)!}{(N - n_2 - 1)!} \frac{(Nz - x_2 + 1)_{N - n_2 - 1}}{(Nw - x_1)_{N - n_1 + 1}} \prod_{i=1}^k \frac{(A_i + 1/2 - Nw)_{B_i - A_i}}{(A_i + 1/2 - Nz)_{B_i - A_i}} \\ &= \left(1 + O\left(\frac{1}{N}\right)\right) \frac{1}{w - z} \frac{1}{\sqrt{\Xi_1(w)\Xi_2(z)}} \exp\{N(S_1(w) - S_2(z))\}. \end{aligned}$$

As for the additional summand, using Lemma 6.2 in [Petrov \(2012\)](#), we write

$$\begin{aligned} &-1_{n_2 < n_1} 1_{x_2 \leq x_1} \frac{(x_1 - x_2 + 1)_{n_1 - n_2 - 1}}{(n_1 - n_2 - 1)!} \\ (28) \quad &= -1_{n_2 < n_1} \frac{(N - n_1)!}{(N - n_2 - 1)!} \times \frac{1}{2\pi i} \oint_{\mathcal{C}(\chi_2)} \frac{(z - x_2 + 1)_{N - n_2 - 1}}{(z - x_1)_{N - n_1 + 1}} dz. \end{aligned}$$

Then, scaling the  $z$  variable as above for the double integral ( $\tilde{z} = z/N$ ), and using the fact that

$$\frac{N(N - n_1)!}{(N - n_2 - 1)!} \frac{(Nz - x_2 + 1)_{N - n_2 - 1}}{(Nz - x_1)_{N - n_1 + 1}} = \left(1 + O\left(\frac{1}{N}\right)\right) \frac{\exp\{N(S_1(z) - S_2(z))\}}{\sqrt{\Xi_1(z)\Xi_2(z)}},$$

we complete the proof.  $\square$

<sup>5</sup>We may drag the  $z$  contour slightly to the left of  $\chi_2$  because the integrand has zeroes in  $z$  which allow that; and also drag it to the right of  $b_k$  because the integrand in (13) does not have  $z$  poles to the right of  $B_k - \frac{1}{2}$ .

4.2. *Critical points of the action.* Proposition 4.2 suggests to use the saddle point (steepest descent) approach [e.g., see Okounkov (2002), Section 3] to investigate the asymptotics of the correlation kernel  $K(x_1, n_1; x_2, n_2)$ . The first step is to understand critical points of the action, that is, points where  $S'(w; \chi, \eta) := \frac{\partial}{\partial w} S(w; \chi, \eta) = 0$ . Let us recall the results about critical points obtained in Petrov (2012):

(1) Depending on the global position  $(\chi, \eta)$  inside the limiting polygon  $\mathcal{P}$ , there are either 0 or 1 critical points of the action in the (open) upper half plane  $\mathbb{H}$ .

(2) Points  $(\chi, \eta) \in \mathcal{P}$  for which there exists a nonreal critical point [denote it by  $w(\chi, \eta)$ ] constitute the (open) liquid region  $\mathcal{D} \subset \mathcal{P}$  where asymptotically one sees all three types of lozenges; see Remark 1.1.

(3) As a function of the global position  $(\chi, \eta) \in \mathcal{D}$ ,  $w(\chi, \eta)$  satisfies the algebraic equation (3) and a form of the complex Burgers equation (4).

(4) When  $(\chi, \eta) \in \mathcal{D}$  approaches the frozen boundary curve  $\partial\mathcal{D}$  (which separates the liquid region from frozen facets), the critical point  $w(\chi, \eta) \in \mathbb{H}$  merges with its complex conjugate  $\bar{w}(\chi, \eta)$ . In addition, points  $(\chi, \eta) \in \partial\mathcal{D}$  that are cusps (= turning points), or points where  $\partial\mathcal{D}$  is tangent to a side of the polygon (see Figure 6) correspond to certain more special types of merging of the critical points  $w(\chi, \eta)$  and  $\bar{w}(\chi, \eta)$ , which we do not need to address in our analysis.<sup>6</sup>

Thus, for all  $(\chi, \eta) \in \partial\mathcal{D}$ , the action  $S(w; \chi, \eta)$  has (at least) double critical point  $w(\chi, \eta) \in \mathbb{R}$  which can be taken as a real parameter on the frozen boundary curve. The map  $w^{-1} : \mathbb{R} \rightarrow \partial\mathcal{D}$  is one-to-one and rational; see Petrov (2012), Proposition 2.6.

**PROPOSITION 4.3.** *The map  $w : \mathcal{D} \rightarrow \mathbb{H}$ ,  $(\chi, \eta) \mapsto w(\chi, \eta)$ , is a diffeomorphism.*

**PROOF.** Finding the image of a point  $z \in \mathbb{H}$  under the inverse map  $w^{-1}$  amounts to solving the equation (3)

$$(29) \quad (z - \chi) \prod_{i=1}^k (z - a_i) = (z - \chi + 1 - \eta) \prod_{i=1}^k (z - b_i)$$

for  $\chi$  and  $\eta$ . Since  $z \in \mathbb{H}$  is complex and  $(\chi, \eta)$  must be real, this is actually a pair of real equations. Let us first rewrite (29) as

$$\chi = z \left( 1 - \prod_{i=1}^k \frac{z - b_i}{z - a_i} \right) + (\chi + \eta - 1) \prod_{i=1}^k \frac{z - b_i}{z - a_i}.$$

<sup>6</sup>See the explanation in the proof of Lemma 4.15 that one can choose paths in Figure 10 away from such more special points.

Since the imaginary part of  $\prod_{i=1}^k \frac{z-b_i}{z-a_i}$  is nonzero for  $z \in \mathbb{H}$  (Lemma 4.4 below), one can always solve the equation

$$\Im \chi = \Im \left( z \left( 1 - \prod_{i=1}^k \frac{z-b_i}{z-a_i} \right) + (\chi + \eta - 1) \prod_{i=1}^k \frac{z-b_i}{z-a_i} \right) = 0$$

for  $\chi + \eta - 1$  and thus find a solution  $(\chi, \eta)$  which belongs to  $\mathcal{D}$  because we have a bijection on the boundary  $\partial \mathcal{D}$ . This implies that the map  $w: \mathcal{D} \rightarrow \mathbb{H}$  is bijective.

The map  $w$  is differentiable, and, moreover, the partial derivatives  $w_\chi$  and  $w_\eta$  cannot both be zero inside  $\mathcal{D}$  because of the complex Burgers equation (4). One can also check that the inverse map is differentiable. This concludes the proof.  $\square$

LEMMA 4.4. *Let  $a_1 < b_1 < \dots < a_k < b_k$ ,  $\sum_{i=1}^k (b_i - a_i) = 1$ , be the parameters of the limiting polygon  $\mathcal{P}$ . Then*

$$\Im \left( \prod_{i=1}^k \frac{z-b_i}{z-a_i} \right) \neq 0, \quad z \in \mathbb{H}.$$

PROOF. Observe that the argument of  $\frac{z-b_i}{z-a_i}$  is the angle under which the segment  $[a_i, b_i]$  is seen from the point  $z$ . Thus, the argument of the whole product  $\prod_{i=1}^k \frac{z-b_i}{z-a_i}$  must be strictly between 0 and  $\pi$ , and so the imaginary part of that product cannot vanish.  $\square$

4.3. *Moving the contours.* Our aim in this subsection is to explain how we deform the contours in the double integral in (27) to employ the saddle point analysis.

Let us assume that (not necessarily distinct) limiting global positions  $(\chi_1, \eta_1)$  and  $(\chi_2, \eta_2)$  in (24) belong to the liquid region  $\mathcal{D} \subset \mathcal{P}$ . Denote the corresponding critical points of the action by  $w_j := w\left(\frac{\chi_j}{N}, \frac{\eta_j}{N}\right) \in \mathbb{H}$ ,  $j = 1, 2$ .

The behavior of  $S_{1,2}$  around  $w_{1,2}$  is quadratic because these critical points are simple; see also the proof of Proposition 4.11. Thus there are four curves starting from each point  $w_{1,2}$  along which the imaginary part  $\Im(S_{1,2}(w))$  is constant; see Figure 11. As the new  $w$  contour we choose the counter-clockwise closed contour passing through  $w_1$  composed of two curves with  $\Im(S_1(w) - S_1(w_1)) = 0$  on which  $\Re(S_1(w) - S_1(w_1)) < 0$  for  $w \neq w_1, \bar{w}_1$  (Figure 11, left). The new counter-clockwise  $z$  contour must pass through  $w_2$  and look like the one on Figure 11, right, so on it we will have  $\Re(S_2(z) - S_2(w_2)) > 0$  for  $z \neq w_2, \bar{w}_2$ .

PROPOSITION 4.5. *The  $z$  and  $w$  contours in the double integral in (27) can always be deformed to become the new contours described above (indicated on Fig-*

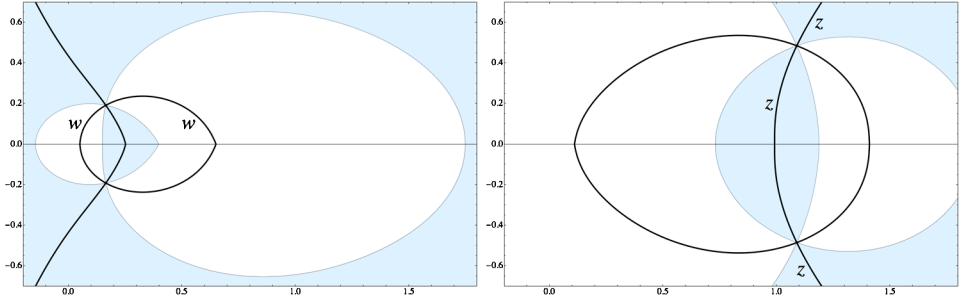


FIG. 11. Critical points  $w_1$  (left) and  $w_2$  (right). Along the bold curves one has  $\Im(S_j(\cdot) - S_j(w_j)) = 0$ ,  $j = 1, 2$ . Shaded are regions where  $\Re(S_j(\cdot) - S_j(w_j)) > 0$ . The new  $w$  and  $z$  contours are indicated on the left and on the right, respectively.

ure 11). This results in the following asymptotics of the kernel  $K$  in the regime (24):

$$(30) \quad K(x_1, n_1; x_2, n_2) = \left(1 + O\left(\frac{1}{N}\right)\right) \frac{1}{2\pi i} \int_{\mathfrak{C}_{\text{single}}} dz \frac{\exp\{N(S_1(z) - S_2(z))\}}{\sqrt{\Xi_1(z)\Xi_2(z)}} + \left(1 + O\left(\frac{1}{N}\right)\right) \frac{1}{(2\pi i)^2} \oint_{\{z\}} \oint_{\{w\}} \frac{dz dw \exp\{N(S_1(w) - S_2(z))\}}{w - z \sqrt{\Xi_1(w)\Xi_2(z)}},$$

where in the double integral  $\{z\}$  and  $\{w\}$  are the new deformed contours.

The single integral may or may not be present; this depends on whether the new contours intersect, and also on the inequality between  $n_1$  and  $n_2$ . All these cases can be unified by choosing an appropriate contour  $\mathfrak{C}_{\text{single}}$ ; see Section 4.4.

PROOF. Let us fix any  $(\chi, \eta) \in \mathcal{D}$ , and set  $w := w(\chi, \eta)$  and  $S(z) := S(z; \chi, \eta)$ . As our *first step*, we aim to justify that the picture of shaded regions where  $\Re(S(z) - S(w)) > 0$  looks exactly as in Figure 11, and also describe the points where the four contours  $\{z : \Im S(z) = \Im S(w)\}$  intersect the real line.

Because  $\Re S(z; \chi, \eta) \sim \eta \ln |z|$  as  $|z| \rightarrow \infty$ , and  $0 < \eta < 1$  inside  $\mathcal{D}$ , far away on Figure 11 we see a shaded region, that is, where  $\Re(S(z) - S(w)) > 0$ .

Since  $S(z)$  is holomorphic everywhere in  $\mathbb{H}$ , along each of the four contours  $\{z : \Im S(z) = \Im S(w)\}$  (the thick curves on Figure 11) the sign of  $\Re(S(z) - S(w))$  must be constant. This implies that each thick curve on Figure 11 from  $w$  to  $\bar{w}$  must be completely inside a shaded or nonshaded region.

Now let us look at the function  $\Im(S(z) - \Im S(w))$  for  $z \in \mathbb{R} + i\varepsilon$  for fixed small  $\varepsilon > 0$ . Observe that

$$\Im((t + i\varepsilon) \ln(t + i\varepsilon)) = \varepsilon \ln |t + i\varepsilon| + t \arg(t + i\varepsilon) \sim \pi \cdot (t)_- := \pi \cdot t 1_{t < 0},$$

where  $t \in \mathbb{R}$ , as  $\varepsilon \rightarrow 0+$ . Thus

$$\frac{1}{\pi} \Im S(t + i\varepsilon) \sim (t - \chi)_- - (t - \chi + 1 - \eta)_- + \sum_{j=1}^k [(b_j - t)_- - (a_j - t)_-];$$

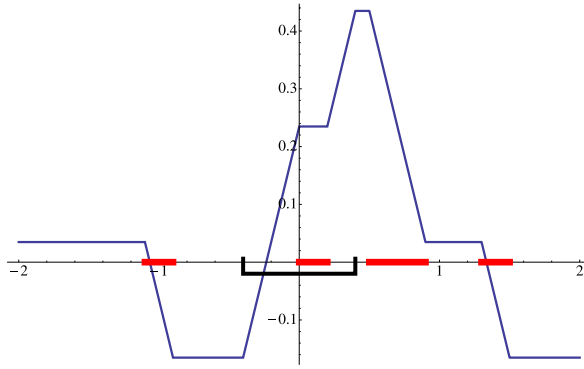


FIG. 12. Graph of  $\frac{1}{\pi} \Im(S(t + i\varepsilon) - S(w))$ ,  $t \in \mathbb{R}$ , for small  $\varepsilon > 0$ . The segments  $[a_j, b_j]$  (red) and  $[\chi + \eta - 1, \chi]$  (black) are displayed.

see Figure 12. Clearly,  $\frac{\partial}{\partial t} \frac{1}{\pi} \Im S(t + i\varepsilon) \sim 1_{t \in [\chi + \eta - 1, \chi]} - \sum_{j=1}^k 1_{t \in [a_j, b_j]}$ . Looking at the slopes of the graph in Figure 12, we see that the four contours  $\{z : \Im S(z) = \Im S(w)\}$  can intersect the real line in at most three points.<sup>7</sup> Because of the relation between these contours and the shaded regions in Figure 11 explained above, there are exactly three such points of intersection:

- $t^+ \in [\chi + \eta - 1, \chi]$ , where  $\Im S(t^+) = \Im S(w)$  and  $\Re S(t^+) > \Re S(w)$ ;
- $t_l^- < t_r^-$ , both belonging to the union of the segments  $[a_j, b_j]$ , where  $\Im S(t_{l,r}^-) = \Im S(w)$  and  $\Re S(t_{l,r}^-) < \Re S(w)$ .

Moreover, from Figure 12 we see that  $t_l^- < t^+ < t_r^-$ . The fourth contour  $\{z : \Im S(z) = \Im S(w)\}$  [with  $\Re S(z) > \Re S(w)$ ] runs to infinity; see Figure 11.

Now as a *second step*, we explain how we can move the  $z$  and  $w$  contours in the double contour integral in (27) to get (30). Looking at the poles in  $z$  and  $w$  in the original integrand in (13), we see that:

- We can drag the points of intersection of the  $z$  contour with  $\mathbb{R}$  (without picking any residues) everywhere except in regions where the slope of the graph on Figure 12 is strictly negative.
- The same goes for the  $w$  contour: we cannot drag it through regions where the slope of the graph on Figure 12 is strictly positive.

The old  $z$  and  $w$  contours are described in Proposition 4.2; together with what was said above, we see that these  $z$  and  $w$  contours can always be deformed in a desired way. The new  $w$  contour will intersect the real line at points  $t_{l,r}^-(\chi_1, \eta_1)$ ;

<sup>7</sup>In fact, the case when there are infinitely many such points (i.e., when a horizontal part of the graph in Figure 12 is lying at the horizontal coordinate line) corresponds to  $(\chi, \eta)$  belonging to the frozen boundary, when the action has a real double critical point; see Section 4.2.

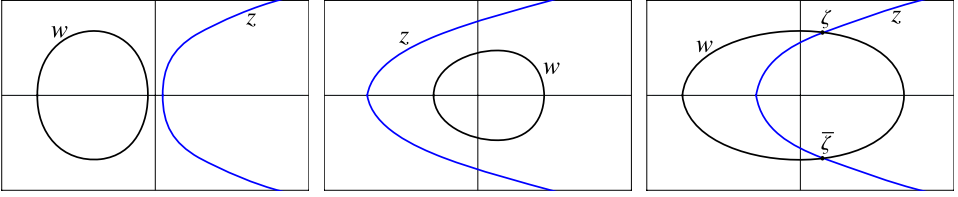


FIG. 13. Various possibilities for the new deformed  $z$  and  $w$  contours.

the new  $z$  contour—at  $t^+(\chi_2, \eta_2)$ . Because the integrand in (13) is regular in  $z$  at  $z = \infty$ , we can let the  $z$  contour pass through infinity.

In the course of this deformation no residues coming from poles on  $\mathbb{R}$  will be picked. However, if the new  $z$  and  $w$  contours intersect, the residue at  $w = z$  will be picked from the  $w$  integral, and then this residue will be integrated in  $z$  over an appropriate arc. Together with the single integral already present in (27), this will lead to appearance of the single integral in (30). We will describe and investigate it in Section 4.4 below.  $\square$

**4.4. Estimating the single integral.** The goal of this subsection is to asymptotically estimate the single integral in (30). A priori from the proof of Proposition 4.5 we see that the integral over  $\mathfrak{C}_{\text{single}}$  may look as follows [we omit the factor  $(1 + O(\frac{1}{N}))$  and the integrand  $\frac{1}{2\pi i} \frac{\exp\{N(S_1(z) - S_2(z))\}}{\sqrt{\mathfrak{E}_1(z)\mathfrak{E}_2(z)}} dz$ ]:

(a) If the new  $z$  and  $w$  contours of Proposition 4.5 do not intersect, then the integral has the form  $1_{n_2 \geq n_1} \oint_{\{z\}}$ , where  $\{z\}$  is the full new  $z$  contour.

(b) If the new contours intersect at points  $\zeta \in \mathbb{H}$  and  $\bar{\zeta}$ , then the integral has the form  $-1_{n_2 < n_1} \int_{\mathfrak{C}_L(\zeta)} + 1_{n_2 \geq n_1} \int_{\mathfrak{C}_R(\zeta)}$ , where  $\mathfrak{C}_L(\zeta)$  is the left part of the new  $z$  contour passed from  $\zeta$  to  $\bar{\zeta}$ , and  $\mathfrak{C}_R(\zeta)$  is its right part passed from  $\bar{\zeta}$  through  $\infty$  to  $\zeta$ .

See Figure 13 for the possible configurations of contours.

**REMARK 4.6.** If the new  $z$  and  $w$  contours intersect more than once in  $\mathbb{H}$ , then the contour  $\mathfrak{C}_{\text{single}}$  would contain several parts. However, then we always can write an estimate of the form

$$\int_{\mathfrak{C}_{\text{single}}} |\cdots| dz \leq 1_{n_2 < n_1} \int_{\mathfrak{C}_L(\zeta)} |\cdots| dz + 1_{n_2 \geq n_1} \int_{\mathfrak{C}_R(\zeta')} |\cdots| dz$$

(dots mean the integrand), where  $\zeta$  and  $\zeta'$  are some points of intersection of the new contours. Below (in Lemmas 4.8 and 4.9 and Proposition 4.10) we estimate the above two summands separately, so we may think that the case (b) covers all possibilities when the two contours intersect.

First, we deal with the case (a):

LEMMA 4.7. *If the new  $z$  and  $w$  contours do not intersect, then there is in fact no single integral in (30).*

PROOF. Recall that the single integral in (30) in that case is asymptotically equivalent to (see Proposition 4.2)

$$1_{n_2 \geq n_1} \frac{1}{2\pi i} \oint_{\{z\}} \frac{N(N-n_1)!}{(N-n_2-1)!} \frac{(Nz-x_2+1)_{N-n_2-1}}{(Nz-n_1+1)} dz.$$

Here  $\{z\}$  is the full new  $z$  contour. This integral can be explicitly computed using Lemma 6.2 in Petrov (2012) [see also (28)], it is equal to

$$1_{n_2 \geq n_1} 1_{x_2 \leq x_1} \frac{(n_1 - n_2)_{x_1 - x_2}}{(x_1 - x_2)!}.$$

This expression is nonzero only if  $x_1 + n_1 \leq x_2 + n_2$ ; otherwise the Pochhammer symbol vanishes. But observe that the three inequalities

$$n_2 \geq n_1, \quad x_2 \leq x_1, \quad x_1 + n_1 \leq x_2 + n_2$$

in the regime (24) imply that (for large  $N$ ) the segment  $[\chi_2 + \eta_2 - 1, \chi_2]$  is completely inside  $[\chi_1 + \eta_1 - 1, \chi_1]$ . From the proof of Proposition 4.5 it follows that the new  $z$  contour crosses the real line at some point inside  $[\chi_2 + \eta_2 - 1, \chi_2]$  (and hence inside  $[\chi_1 + \eta_1 - 1, \chi_1]$ ), and the new  $w$  contour passes through two real points at the opposite sides of  $[\chi_1 + \eta_1 - 1, \chi_1]$ . Thus, we see that in this situation the new  $z$  and  $w$  contours must intersect. This concludes the proof.  $\square$

Now we will obtain certain estimates in the case (b).

LEMMA 4.8. *Let  $n_2 \geq n_1$ , and  $\mathfrak{C}_R(\zeta)$  for  $\zeta \in \mathbb{H}$  be defined as above. We have the estimate*

$$\left| \frac{1}{2\pi i} \int_{\mathfrak{C}_R(\zeta)} \frac{\exp\{N(S_1(z) - S_2(z))\}}{\sqrt{\mathfrak{E}_1(z)\mathfrak{E}_2(z)}} dz \right| \leq C \exp\{N \cdot \Re(S_1(\zeta) - S_2(\zeta))\}.$$

Here the constant  $C$  is uniform for  $(x_1, n_1), (x_2, n_2)$  in the regime (24) with the condition  $n_2 \geq n_1$ , for the limiting global positions  $(\chi_1, \eta_1), (\chi_2, \eta_2)$  belonging to a compact region  $\mathcal{D}_c \subset \mathcal{D}$ .

PROOF. Assume first that  $(x_1, n_1) \neq (x_2, n_2)$ . For large  $|z|$ , we have the expansion

$$\begin{aligned} F(z) &:= S_1(z) - S_2(z) \\ &= \text{const} + \frac{n_1 - n_2}{N} \ln z \\ &\quad + \frac{1}{z} \left( \frac{n_2^2 - n_1^2}{2N^2} + \left(1 - \frac{x_2}{N}\right) \left(1 - \frac{n_2}{N}\right) - \left(1 - \frac{x_1}{N}\right) \left(1 - \frac{n_1}{N}\right) \right) \\ &\quad + O\left(\frac{1}{z^2}\right). \end{aligned}$$

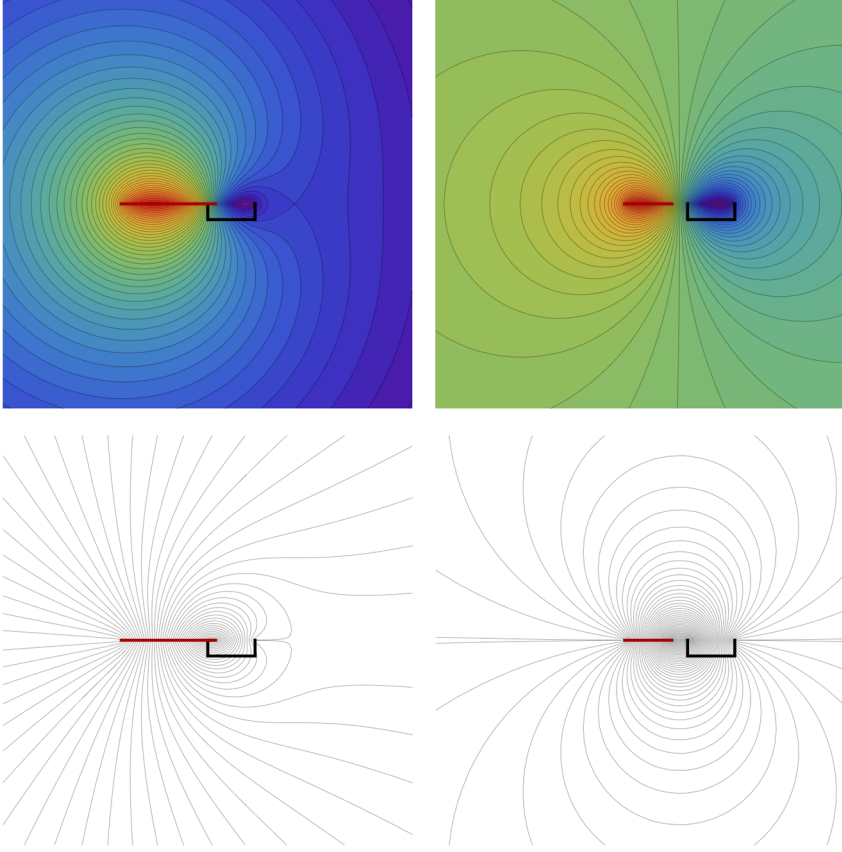


FIG. 14. Level lines of  $\Re F(z)$  (top; warmer colors represent larger values) and  $\Im F(z)$  (bottom) in the case  $n_2 \geq n_1$  (left) and  $n_2 = n_1$  (right). The red (left) segment is  $[\chi_1 + \eta_1 - 1, \chi_1]$ , and the black (right) one is  $[\chi_2 + \eta_2 - 1, \chi_2]$ .

Observe that the function  $F(z)$  has no nonreal critical points. This implies that there is a curve in  $\mathbb{H}$  starting at the point  $\zeta \in \mathbb{H}$  along which  $\Im F(z) = \Im F(\zeta)$  and  $\Re F(z) < \Re F(\zeta)$  for  $z \neq \zeta$ . This curve can either extend to infinity, or cross the real line somewhere in the segment  $[\chi_2 + \eta_2 - 1, \chi_2]$ ; see Figure 14. This can be seen by considering the function  $\Im F(t + i\varepsilon)$  of  $t \in \mathbb{R}$  similarly to the proof of Proposition 4.5. Note that for  $n_2 = n_1$ , such curves will never to go to infinity (Figure 14, right). In the lower half plane the situation is symmetric.

Since the integrand is regular at  $z = \infty$  (see the proof of Proposition 4.2), we can always transform the contour  $\mathcal{C}_R(\zeta)$  so that it will consist of curves described above [along which  $\Re F(z) < \Re F(\zeta)$ ]. This implies the claim for  $(x_1, n_1) \neq (x_2, n_2)$  because if  $(\chi_j, \eta_j) \in \mathcal{D}_c$ , then the factor  $1/\sqrt{\Xi_1(z)\Xi_2(z)}$  in the integrand is uniformly bounded. For  $(x_1, n_1) = (x_2, n_2)$ , the integral does not depend on  $N$ , and the claim is trivial.  $\square$



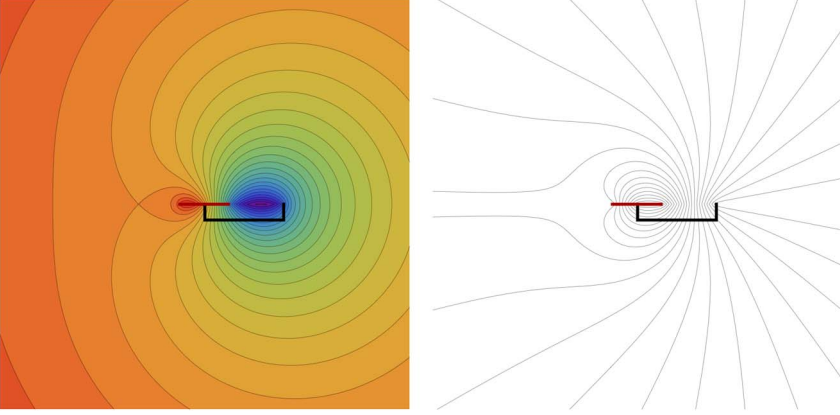


FIG. 15. Level lines of  $\Re F(z)$  (left; warmer colors represent larger values) and  $\Im F(z)$  (right) in the case  $n_2 < n_1$ .

LEMMA 4.9. Let  $n_2 < n_1$ , and  $\mathfrak{C}_L(\zeta)$  for  $\zeta \in \mathbb{H}$  be defined as above. We have

$$\left| \frac{1}{2\pi i} \int_{\mathfrak{C}_L(\zeta)} \frac{\exp\{N(S_1(z) - S_2(z))\}}{\sqrt{\mathfrak{E}_1(z)\mathfrak{E}_2(z)}} dz \right| \leq C \exp\{N \cdot \Re(S_1(\zeta) - S_2(\zeta))\}.$$

Here the constant  $C$  is uniform for  $(x_1, n_1), (x_2, n_2)$  in the regime (24) with the condition  $n_2 < n_1$ , for the limiting global positions  $(\chi_1, \eta_1), (\chi_2, \eta_2)$  belonging to a compact region  $\mathcal{D}_c \subset \mathcal{D}$ .

PROOF. This is established in the same way as Lemma 4.8. Since  $\mathfrak{C}_L(\zeta)$  never extends to infinity, we can always transform it to get the desired estimate; see Figure 15.  $\square$

From Lemmas 4.8 and 4.9 we derive a stronger estimate which we will use:

PROPOSITION 4.10. The single integral in (30) can be estimated as

$$(31) \quad \left| \frac{1}{2\pi i} \int_{\mathfrak{C}_{\text{single}}} \frac{\exp\{N(S_1(z) - S_2(z))\}}{\sqrt{\mathfrak{E}_1(z)\mathfrak{E}_2(z)}} dz \right| \leq \frac{C \exp\{N \cdot \Re(S_1(\zeta) - S_2(\zeta))\}}{1 + R},$$

where  $R := \sqrt{(x_1 - x_2)^2 + (n_1 - n_2)^2}$ . The constant  $C$  is uniform for  $(x_1, n_1)$  and  $(x_2, n_2)$  behaving as in (24), for the limiting global positions  $(\chi_1, \eta_1), (\chi_2, \eta_2)$  belonging to a compact region  $\mathcal{D}_c \subset \mathcal{D}$ .

PROOF. The passage from the estimates of Lemmas 4.8 and 4.9 to (31) is done similarly to Duits (2011), Lemma 6.3, and is based on a standard steepest descent argument.

Let  $\zeta \in \mathbb{H}$  be the point of intersection of the  $z$  and  $w$  contours of Proposition 4.5 (see also Figure 13) where the contour  $\mathcal{C}_{\text{single}}$  starts. (If the  $z$  and  $w$  contours do not intersect, the claim is trivial by Lemma 4.7.) Assume that we have transformed  $\mathcal{C}_{\text{single}}$  as in Lemma 4.8 or 4.9 so that on it we have  $\Im F(z) = \Im F(\zeta)$  and  $\Re F(z) < \Re F(\zeta)$  for  $z \neq \zeta$ , where  $F(z) = S_1(z) - S_2(z)$ . If the new contour extends to infinity (Figure 14, left), let us close it so that it will become bounded. Denote this new contour by  $\mathcal{C}'_{\text{single}}$ .

Let us choose a smooth parametrization  $z = z(t)$  of the part of the curve  $\mathcal{C}'_{\text{single}}$  inside  $\mathbb{H}$  such that  $z(0) = \zeta$  and  $z(1) \in \mathbb{R}$ . We have  $|z'(t)| < \text{const}$  [and by compactness of  $\mathcal{D}_c$  this constant is uniform in  $(x_j, n_j)$ ], so

$$\left| \frac{1}{2\pi i} \int_{\mathcal{C}'_{\text{single}}} \frac{\exp\{N(S_1(z) - S_2(z))\}}{\sqrt{\Xi_1(z)\Xi_2(z)}} dz \right| \leq \text{const} \cdot \int_0^1 \exp\{N \cdot \Re(F(z(t)))\} dt.$$

Let us assume that  $(x_1, n_1) \neq (x_2, n_2)$ ; otherwise the claim is again trivial. We have

$$(x_1 - x_2, n_1 - n_2) = R(\cos \phi, \sin \phi), \quad R > 0.$$

Denote

$$N \cdot \Re(F(z(t))) = R \cdot G_{1,2}(t; \phi).$$

The property that  $\Re F(z) < \Re F(\zeta)$  on our contour allows to write the following estimate. Since  $\mathcal{D}_c$  is compact and  $\zeta$  depends continuously on  $(\chi_j, \eta_j)$ , we can choose  $r > 0$  uniformly so that

$$G_{1,2}(t; \phi) - G_{1,2}(0; \phi) < -At, \quad 0 \leq t \leq r,$$

with a constant  $A$  not depending on  $\zeta$  or  $\phi$ .

Then we have

$$\begin{aligned} \int_0^r e^{RG_{1,2}(t; \phi)} dt &= e^{RG_{1,2}(0; \phi)} \int_0^r e^{R(G_{1,2}(t; \phi) - G_{1,2}(0; \phi))} dt \\ &\leq e^{RG_{1,2}(0; \phi)} \int_0^r e^{-ARt} dt \leq \frac{1}{AR} e^{RG_{1,2}(0; \phi)} \end{aligned}$$

and

$$\int_r^1 e^{RG_{1,2}(t; \phi)} dt \leq e^{-ArR} e^{RG_{1,2}(0; \phi)},$$

because on the contour  $\{z(t) : r \leq t \leq 1\}$  we have the inequalities  $\Re F(z) \leq \Re F(z(r)) \leq \Re F(\zeta) - Ar$ . This concludes the proof.  $\square$

**4.5. Asymptotics of the kernel in the bulk.** Our aim in this subsection is to write an exact asymptotic expansion of the kernel  $K(x_1, n_1; x_2, n_2)$  (30) when the two points  $(x_1, n_1)$  and  $(x_2, n_2)$  are in the bulk of the system [i.e., they behave as in (24) and  $(\chi_j, \eta_j) \in \mathcal{D}$ ] and are sufficiently far from each other. The technique of getting such an expansion involves only “local” properties of the double

contour integral formula (30) for the kernel (in contrast to some considerations of Section 4.4), and mainly follows the approach of Borodin and Ferrari (2008) and Duits (2011).

PROPOSITION 4.11. *Fix (sufficiently small)  $\delta > 0$  and a compact  $\mathcal{D}_c \subset \mathcal{D}$ . Uniformly in  $(x_j, n_j)$  ( $j = 1, 2$ ) with  $(\frac{x_j}{N}, \frac{n_j}{N}) \in \mathcal{D}_c$ , such that  $\|(x_1, n_1) - (x_2, n_2)\| \geq N^{1/2+\delta}$ , we have the following expansion:*

$$\begin{aligned}
 & K(x_1, n_1; x_2, n_2) \\
 &= -\frac{1}{2\pi N} \left( \frac{e^{N(S_1(w_1) - S_2(w_2))}}{(w_1 - w_2)\sqrt{\Xi_1(w_1)\Xi_2(w_2)}(-S_1''(w_1))^{1/2}(S_2''(w_2))^{1/2}} \right. \\
 &\quad + \frac{e^{N(S_1(\bar{w}_1) - S_2(w_2))}}{(\bar{w}_1 - w_2)\sqrt{\Xi_1(\bar{w}_1)\Xi_2(w_2)}(-S_1''(\bar{w}_1))^{1/2}(S_2''(w_2))^{1/2}} \\
 &\quad + \frac{e^{N(S_1(w_1) - S_2(\bar{w}_2))}}{(w_1 - \bar{w}_2)\sqrt{\Xi_1(w_1)\Xi_2(\bar{w}_2)}(-S_1''(w_1))^{1/2}(S_2''(\bar{w}_2))^{1/2}} \\
 &\quad \left. + \frac{e^{N(S_1(\bar{w}_1) - S_2(\bar{w}_2))}}{(\bar{w}_1 - \bar{w}_2)\sqrt{\Xi_1(\bar{w}_1)\Xi_2(\bar{w}_2)}(-S_1''(\bar{w}_1))^{1/2}(S_2''(\bar{w}_2))^{1/2}} \right) \\
 &\quad \times (1 + O(N^{-\delta/2})).
 \end{aligned} \tag{32}$$

The branches of the square roots  $(\pm S_j''(\dots))^{1/2}$  above are chosen in accordance with the directions of the  $w$  and  $z$  contours in the double integral in (30) at points  $w_1, \bar{w}_1$  and  $w_2, \bar{w}_2$ , respectively; see (34) in the proof.

PROOF. Observe that the contribution from the single integral in (30) given in Proposition 4.10 is asymptotically negligible in comparison to the desired expansion (32). Thus, it suffices to consider only the double contour integral in (30),

$$(33) \quad I_2(x_1, n_1; x_2, n_2) := \frac{1}{(2\pi i)^2} \oint_{\{z\}} \oint_{\{w\}} \frac{dz dw \exp\{N(S_1(w) - S_2(z))\}}{w - z \sqrt{\Xi_1(w)\Xi_2(z)}}.$$

Recall that the  $w$  contour passes through the critical points  $w_1, \bar{w}_1$ , and on it we have  $\Im S_1(w) = \Im S_1(w_1)$  and  $\Re S_1(w) < \Re S_1(w_1)$  for  $w \neq w_1, \bar{w}_1$ . Similarly for the  $z$  contour: it passes through  $w_2, \bar{w}_2$ , and on it  $\Im S_2(z) = \Im S_2(w_2)$ , and  $\Re S_2(z) > \Re S_2(w_2)$  for  $z \neq w_2, \bar{w}_2$ .

The main contributions to (33) come from neighborhoods of the critical points, and parts of the contours which are sufficiently far from them give an exponentially small contribution. Since there are four pairs of critical points, we get four summands in (32). Let us consider only the case of  $(w_1, w_2)$ , for the other three pairs the situation is analogous.

In small neighborhoods of  $w_1$  and  $w_2$  let us replace the (curved)  $w$  and  $z$  contours by the corresponding tangent lines. Introduce the local coordinates  $t, s \in$

$[-N^\delta, N^\delta]$  as follows:

$$(34) \quad w(t) = w_1 + \frac{t}{\sqrt{N}(-S_1''(w_1))^{1/2}}, \quad z(s) = w_2 + \frac{s}{\sqrt{N}(S_2''(w_2))^{1/2}}.$$

Here the branches of the square roots  $(-S_1''(w_1))^{1/2}$  and  $(S_2''(w_2))^{1/2}$  are chosen so that when  $t$  (resp.,  $s$ ) increases, the point  $w(t)$  [resp.,  $z(s)$ ] passes along the tangent line to the  $w$  (resp.,  $z$ ) contour in the direction of that contour.

In these new variables the behavior of the exponents in the double contour integral is

$$(35) \quad \begin{aligned} \lim_{N \rightarrow \infty} N(S_1(w(t)) - S_1(w_1)) &= -t^2/2, \\ \lim_{N \rightarrow \infty} N(S_2(z(s)) - S_2(w_2)) &= s^2/2. \end{aligned}$$

The convergence here is uniform for  $t, s \in [-N^\delta, N^\delta]$  and also (by compactness of  $\mathcal{D}_c$  and continuity) for our values of  $(x_j, n_j)$ . Moreover, at the endpoints  $t, s = \pm N^\delta$  the expressions  $e^{N(S_1(w(t)) - S_1(w_1))}$  and  $e^{N(S_2(z(s)) - S_2(w_2))}$  are exponentially small. Parts of the contours which are even farther from the critical points  $w_1, \bar{w}_1$  and  $w_2, \bar{w}_2$  thus give an exponentially negligible contribution.

This implies that the double contour integral (33) picks the following contribution from the neighborhood of  $(w_1, w_2)$ :

$$(36) \quad \begin{aligned} &\frac{1}{(2\pi i)^2} \frac{1}{N(-S_1''(w_1))^{1/2}(S_2''(w_2))^{1/2}} \int_{-N^\delta}^{N^\delta} \int_{-N^\delta}^{N^\delta} ds dt \\ &\times \frac{\exp\{N(S_1(w(t)) - S_2(z(s)))\}}{(w(t) - z(s))\sqrt{\Xi_1(w(t))\Xi_2(z(s))}}. \end{aligned}$$

Let us now get rid of nonexponential terms in the integral above. The map  $w^{-1} : \mathbb{H} \rightarrow \mathcal{D}$  is a diffeomorphism, so there exists a constant  $A > 0$  such that

$$|w_1 - w_2| \geq A \|(\chi_1, \eta_1) - (\chi_2, \eta_2)\| \geq AN^{-1/2+\delta}.$$

The second derivatives  $S_{1,2}''(w_{1,2})$  are nonzero inside  $\mathcal{D}$  and hence are bounded from below in  $\mathcal{D}_c$  (recall that they vanish on the frozen boundary  $\partial\mathcal{D}$ ). Thus, we may write

$$\frac{1}{w(t) - z(s)} = \frac{1}{w_1 - w_2} (1 + O(N^{-\delta/2})),$$

where the constant in  $O(N^{-\delta/2})$  does not depend on  $\delta$  (it depends only on  $\mathcal{D}_c$ ). We can also replace  $\Xi_1(w(t))\Xi_2(z(s))$  by  $\Xi_1(w_1)\Xi_2(w_2)$ . This will affect the asymptotics by a factor which is less significant than  $(1 + O(N^{-\delta/2}))$ . Thus, we may

rewrite (36) as

$$\frac{1}{(2\pi)^2} \frac{e^{N(S_1(w_1) - S_2(w_2))}}{N(-S_1''(w_1))^{1/2}(S_2''(w_2))^{1/2}(w_1 - w_2)\sqrt{\Xi_1(w_1)\Xi_2(w_2)}} \\ \times (1 + O(N^{-\delta/2})) \int_{-N^\delta}^{N^\delta} \int_{-N^\delta}^{N^\delta} e^{N(S_1(w(t)) - S_1(w_1) - S_2(z(s)) + S_2(w_2))} ds dt.$$

Taking  $N$  large and using the uniform asymptotics (35), we see that the above double integral becomes Gaussian and can be explicitly evaluated. This completes the proof.  $\square$

**COROLLARY 4.12.** *In the setting of Proposition 4.11, we have the same expansion for  $K(x_1, n_1; x_2 + 1, n_2 - 1)$  as in (32), but with an extra factor of  $\frac{w_2 - x_2/N}{1 - n_2/N}$  in each term with  $w_2$ , and with a factor of  $\frac{\bar{w}_2 - x_2/N}{1 - n_2/N}$  in each term with  $\bar{w}_2$ .*

**PROOF.** This is obtained in the same way as Proposition 4.11 using the fact that

$$-NS\left(z; \frac{x_2 + 1}{N}, \frac{n_2 - 1}{N}\right) \sim -NS\left(z; \frac{x_2}{N}, \frac{n_2}{N}\right) - \ln\left(1 - \frac{n_2}{N}\right) + \ln\left(z - \frac{x_2}{N}\right).$$

See also Lemma 7.4 in Petrov (2012).  $\square$

We can also write an estimate of the double contour integral  $I_2$  (33) when the points  $(x_1, n_1)$  and  $(x_2, n_2)$  are sufficiently close:

**LEMMA 4.13.** *Fix (sufficiently small)  $\delta > 0$  and a compact  $\mathcal{D}_c \subset \mathcal{D}$ . Uniformly in  $(x_j, n_j)$  ( $j = 1, 2$ ) with  $(\frac{x_j}{N}, \frac{n_j}{N}) \in \mathcal{D}_c$ , such that  $\|(x_1, n_1) - (x_2, n_2)\| \leq N^{1/2+\delta}$ , we have the following estimate:*

$$|I_2(x_1, n_1; x_2, n_2)| \leq \frac{C e^{N \cdot \Re(S_1(w_1) - S_2(w_2))}}{\sqrt{N}}.$$

**PROOF.** We argue as in Proposition 4.11, but now we must estimate the term  $1/(w(t) - z(s))$  in a different way. Since the points  $w_1$  and  $w_2$  are close, we can write  $S_1''(w_1) = S_2''(w_2)(1 + O(N^{-1/2+\delta}))$ , where the constant in  $O(N^{-1/2+\delta})$  is uniform in our  $(x_j, n_j)$ 's and depends only on  $\mathcal{D}_c$ . This implies that in  $1/(w(t) - z(s))$  we can replace  $(-S_1''(w_1))^{1/2}$  with  $\pm i(S_2''(w_2))^{1/2}$ , where the sign  $\pm$  depends on the choice of square roots. Moreover, we have  $|w_1 - w_2| = O(N^{-1/2+\delta})$ , so we can write

$$\frac{1}{w(t) - z(s)} \approx \frac{\sqrt{N}}{\sqrt{N}(w_1 - w_2) - (S_2''(w_2))^{-1/2}(s \pm it)}.$$

Then we proceed as in the proof of Proposition 4.11 and see that the resulting double integral has the following asymptotics coming from the neighborhood of  $(w_1, w_2)$ :

$$\begin{aligned} & \frac{1}{(2\pi)^2} \frac{e^{N(S_1(w_1) - S_2(w_2))}}{\sqrt{N}(-S_1''(w_1))^{1/2}(S_2''(w_2))^{1/2}\sqrt{\Xi_1(w_1)\Xi_2(w_2)}} \\ & \times \int_{-N^\delta}^{N^\delta} \int_{-N^\delta}^{N^\delta} \frac{e^{N(S_1(w(t)) - S_1(w_1) - S_2(z(s)) + S_2(w_2))}}{\sqrt{N}(w_1 - w_2) - (S_2''(w_2))^{-1/2}(s \pm it)} ds dt. \end{aligned}$$

(For other three pairs of critical points, one can get the same estimate.) Depending on how close the points  $w_1$  and  $w_2$  in our regime, we see that the above integral may have a singularity which is integrable, and (on the other hand) the expression  $\sqrt{N}(w_1 - w_2)$  may go to infinity. This implies that we can always bound the integral by a constant, and thus we arrive at the desired estimate.  $\square$

REMARK 4.14. In Proposition 4.11 we see that when the points  $(x_j, n_j)$  ( $j = 1, 2$ ) are sufficiently far from each other, the main contribution to  $K(x_1, n_1; x_2, n_2)$  (30) comes from the double contour integral. On the contrary, for sufficiently close points  $(x_j, n_j)$ , the single integral in (30) is asymptotically more significant. On the extreme, when asymptotically the differences  $x_1 - x_2, n_1 - n_2 \in \mathbb{Z}$  stabilize, the double integral in (30) vanishes in the limit, while the single integral gives rise to the incomplete beta kernel; see Petrov [(2012), Theorem 2 and Proposition 7.9].

4.6. *Estimates of the kernel close to the edge and in the facet.* We conclude this section with several estimates for the kernel  $K(x_1, n_1; x_2, n_2)$  (30) when one or both points  $(x_j, n_j)$  becomes close to the lower left edge of the liquid region  $\mathcal{D}$ , or outside  $\mathcal{D}$  in the lower left facet; see Figure 10. We mainly follow a similar treatment for a simpler kernel which was performed in Borodin and Ferrari (2008), Section 6.

Recall (Section 3.2) that we choose the paths for calculating the height function as in Figure 10 ending in the lower left facet. Let  $\eta = \eta_{\text{fb}}(\chi)$  be the equation for the corresponding lower left part of the frozen boundary. Thus, the liquid region (sufficiently close to that part of  $\partial\mathcal{D}$ ) is determined by the inequality  $\eta - \eta_{\text{fb}}(\chi) > 0$ . We distinguish three regimes for a point  $(x, n)$  (in the pre-limit integer coordinates):

$$(37) \quad (\text{inside the liquid region}) \quad n - N\eta_{\text{fb}}(x/N) \geq N^{2/3};$$

$$(38) \quad (\text{close to the edge}) \quad N^{2/3} \geq n - N\eta_{\text{fb}}(x/N) \geq cN^{1/3};$$

$$(39) \quad (\text{at the edge or in the facet}) \quad n - N\eta_{\text{fb}}(x/N) \leq cN^{1/3}$$

for some  $c > 0$ .

LEMMA 4.15. *Assume that the points  $(x_j, n_j)$  ( $j = 1, 2$ ) behave as in (24), and one or both of them is close to the lower left edge as in (38). Also, let  $|w_1 -$*

$w_2|$  be bounded away from zero uniformly in  $N$ . Then there exists  $c$  in (38) large enough so that we have

$$(40) \quad |K(x_1, n_1; x_2, n_2)| \leq \frac{C e^{N\Re(S_1(w_1) - S_2(w_2))}}{N \sqrt{|S_1''(w_1) S_2''(w_2)|}},$$

uniformly in  $N$ .

PROOF. Because  $|w_1 - w_2|$  must be bounded from below, we see that the limiting global positions  $(\chi_j, \eta_j)$ ,  $j = 1, 2$ , must be distinct. Proposition 4.10 (cf. Remark 4.14) then implies that the single integral in (30) is asymptotically less significant than the desired estimate (40) for the kernel [note that at least one of the factors  $S_1''(w_1)$ ,  $S_2''(w_2)$  goes to zero as  $N \rightarrow \infty$ , see also the proof of Lemma 5.2]. Therefore, it suffices to derive (40) for the double contour integral in (30).

As usual in the steepest descent approach, the main contribution to the double contour integral in (30) comes from the neighborhoods of the critical points. Thus, there we have  $w \approx w_1$ ,  $z \approx w_2$  (plus three more possibilities with  $\bar{w}_{1,2}$  replacing  $w_{1,2}$ , but they give the same contribution to the desired bound).

Let, by agreement, the paths in Figure 10 be separated [in the limiting coordinates  $(\chi, \eta)$ ] form the tangent points of the frozen boundary and the sides of the polygon. Clearly, such paths still can be chosen. Thus, we may think that the quantities  $\Xi_1(w_1)$  and  $\Xi_2(w_2)$  are uniformly bounded away from zero; see also Petrov (2012), Proposition 2.7 and Figure 14. Thus, it remains to estimate the product of two single integrals

$$\oint_{\{w\}} e^{NS_1(w)} dw \oint_{\{z\}} e^{-NS_2(z)} dz,$$

where the  $w$  and  $z$  contours are as in (30). We will derive the estimate of the form  $\frac{C e^{\pm N\Re S_{1,2}(w_{1,2})}}{\sqrt{N|S_{1,2}''(w_{1,2})|}}$  for each of the single integrals (with “+” sign for the first integral, and “−” for the second one), and this will give the desired claim. If, say,  $(x_1, n_1)$  is not close to the edge, then the corresponding estimate can be obtained in the same way as in Proposition 4.11. So let us assume that  $(x_1, n_1)$  is close to the lower left edge, and estimate the  $w$  integral above; for the  $z$  integral the argument is the same.

From Petrov (2012), Proposition 2.7, it follows that for  $(x_1, n_1)$  approaching the lower left edge of the liquid region, the corresponding critical point  $w_1$  approaches the real line to the left of the point  $a_1$  from (1). Using Petrov (2012), Section 2.3 and (2.10) (cf. Remark 1.1), it can be shown that  $\arg S_1''(w_1)$  tends to  $-\pi/2$ . Let us introduce the local variable  $t$  around  $w_1$ ,

$$w(t) = w_1 + e^{-i\pi/4} t, \quad -\delta \leq t \leq \sqrt{2}\Im(w_1).$$

It can be readily checked [cf. [Borodin and Ferrari \(2008\)](#), Lemma 6.8] that replacing the  $w$  contour around  $w_1$  by the straight line  $\{w(t)\}$  will not affect the desired bound [provided that  $c$  in (38) is large enough]. We then have

$$S_1(w(t)) = S_1(w_1) - \frac{i}{2} S_1''(w_1) t^2 - \frac{1+i}{6\sqrt{2}} S_1'''(w_1) t^3 + O(t^4),$$

and  $\Re(-\frac{i}{2} S_1''(w_1) t^2) \approx -\frac{1}{2} |S_1''(w_1)| t^2$ . Since  $w_1$  is close to the real line, one can derive an equivalence of the form  $S_1'''(w_1) \approx \frac{S_1''(w_1)}{i\Im(w_1)} \approx -\frac{|S_1''(w_1)|}{\Im(w_1)}$ , and so

$$\Re\left(-\frac{1+i}{6\sqrt{2}} S_1'''(w_1) t^3\right) \approx \frac{1}{6\sqrt{2}\Im(w_1)} |S_1''(w_1)| t^3.$$

We see that for  $-\delta \leq t \leq 0$ , the cubic term helps the convergence, and for  $0 \leq t \leq \sqrt{2}\Im(w_1)$ , we can bound the cubic term by the quadratic term which will also ensure the convergence. We thus see that the integral of  $e^{N(S_1(w) - S_1(w_1))}$  around  $w_1$  is equal to a constant times the integral of  $\exp(-\frac{N}{2} |S_1''(w_1)| t^2)$ , which leads to the desired estimate.  $\square$

To describe further estimates, we need to introduce some notation. Let  $(x, n)$  be at the lower left edge or in the corresponding facet as in (39). We would like to mimic the critical point  $w(\frac{x}{N}, \frac{n}{N})$  and the value of the action  $S(w(\frac{x}{N}, \frac{n}{N}); \frac{x}{N}, \frac{n}{N})$  for such  $(x, n)$  as follows:

$$\begin{aligned} \tilde{w} &= \tilde{w}\left(\frac{x}{N}, \frac{n}{N}\right) := w\left(\frac{x}{N}, \eta_{\text{fb}}\left(\frac{x}{N}\right)\right) \in \mathbb{R}, \\ \tilde{S}\left(w; \frac{x}{N}, \frac{n}{N}\right) &:= \left(w - \frac{x}{N}\right) \ln\left(w - \frac{x}{N}\right) \\ &\quad - \left(w - \frac{x}{N} + 1 - \frac{n}{N}\right) \ln\left(w - \frac{x}{N} + 1 - \eta_{\text{fb}}\left(\frac{x}{N}\right)\right) \\ &\quad + \left(1 - \frac{n}{N}\right) \ln\left(1 - \eta_{\text{fb}}\left(\frac{x}{N}\right)\right) \\ &\quad + \sum_{i=1}^k [(b_i - w) \ln(b_i - w) - (a_i - w) \ln(a_i - w)]. \end{aligned}$$

Denote by  $\tilde{w}_{1,2}$  and  $\tilde{S}_{1,2}(w)$  the corresponding quantities at  $(x_{1,2}, n_{1,2})$  similarly to  $w_{1,2}$  and  $S_{1,2}(w)$ ; see also (26). Note that when the point  $(x, n)$  is at the edge, that is, when  $n - N\eta_{\text{fb}}(x/N) = O(N^{1/3})$ , we have  $|w - \tilde{w}| = O(N^{1/3})$ , and same for  $\tilde{S}$ .

**LEMMA 4.16.** *Assume that the situation is as in Lemma 4.15, but now the point  $(x_2, n_2)$  is at the lower left edge or in the corresponding facet as in (39),*



while  $(x_1, n_1)$  is in the bulk (37) or close to the edge (38). Let  $|w_1 - \tilde{w}_2|$  be bounded away from zero uniformly in  $N$ . Then, also uniformly in  $N$ , we get the following estimate with  $C, C_2 > 0$ :

$$\begin{aligned} & |K(x_1, n_1; x_2, n_2)| \\ & \leq \frac{C e^{N\Re S_1(w_1)}}{\sqrt{N|S_1'(w_1)|}} \times \frac{e^{-N\Re \tilde{S}_2(\tilde{w}_2)}}{N^{1/3}} \exp\left\{-C_2 N^{2/3} \left(\eta_{\text{fb}}\left(\frac{x_2}{N}\right) - \frac{n_2}{N}\right)\right\}. \end{aligned}$$

PROOF. Similarly to the beginning of the proof of Lemma 4.15, we see that it suffices to estimate the product of two single integrals. The  $w$  integral is bounded as in Lemma 4.15 (yielding the first factor in the claim). Thus, it remains to estimate the  $z$  integral  $\oint_{\{z\}} e^{-NS_2(z)} dz$ . We will mainly follow the approach of Borodin and Ferrari (2008), Section 6.1 [which is in turn based on the technique first applied in Borodin, Ferrari and Sasamoto (2008), Propositions 15 and 17]. We provide a brief derivation omitting certain bounds which are done in a way similar to what is performed in Borodin and Ferrari (2008), Section 6.1.

Let us first consider the following scaling of  $(x_2, n_2)$ :

$$x_2 = [\chi_2 N], \quad n_2 = [N\eta_{\text{fb}}(\chi_2) + uN^{1/3}],$$

where  $u \in \mathbb{R}$ , and  $\chi_2$  is some coordinate such that the line  $\{\chi : \chi = \chi_2\}$  intersects the lower left part of the frozen boundary as in Figure 10. Let us expand

$$-NS\left(z; \frac{x_2}{N}, \frac{n_2}{N}\right) \approx -NS(z; \chi_2, \eta_{\text{fb}}(\chi_2)) - uN^{1/3}S_\eta(z; \chi_2, \eta_{\text{fb}}(\chi_2)).$$

We deform the  $z$  contour in  $\oint_{\{z\}} e^{-NS_2(z)} dz$  so that it will pass through the real double critical point  $\tilde{w}_2 = w(\chi_2, \eta_{\text{fb}}(\chi_2))$ . As it usually happens for Airy-type asymptotics, the main contribution to the integral comes from an  $N^{1/3}$ -neighborhood of the double critical point. Let us introduce the local variable  $t$ ,

$$z = \tilde{w}_2 + tN^{-1/3},$$

and continue the above expansion,

$$\begin{aligned} & -NS(\tilde{w}_2 + tN^{-1/3}; \chi_2, \eta_{\text{fb}}(\chi_2)) - uN^{1/3}S_\eta(\tilde{w}_2 + tN^{-1/3}; \chi_2, \eta_{\text{fb}}(\chi_2)) \\ & \approx -NS(\tilde{w}_2; \chi_2, \eta_{\text{fb}}(\chi_2)) - \frac{1}{6}t^3S'''(\tilde{w}_2; \chi_2, \eta_{\text{fb}}(\chi_2)) \\ & \quad - uN^{1/3}S_\eta(\tilde{w}_2; \chi_2, \eta_{\text{fb}}(\chi_2)) - utS'_\eta(\tilde{w}_2; \chi_2, \eta_{\text{fb}}(\chi_2)). \end{aligned}$$

The terms  $-\frac{1}{6}t^3S'''(\tilde{w}_2; \chi_2, \eta_{\text{fb}}(\chi_2)) - utS'_\eta(\tilde{w}_2; \chi_2, \eta_{\text{fb}}(\chi_2))$  after the integration in the neighborhood of the double critical point  $\tilde{w}_2$  give the Airy function [similarly to Borodin and Ferrari (2008), Lemma 6.1]. The terms containing  $N$  contribute to the factor  $e^{-N\Re \tilde{S}_2(\tilde{w}_2)}$  [after substituting  $u = N^{2/3}(\frac{n_2}{N} - \eta_{\text{fb}}(\frac{x_2}{N}))$ ].

For general  $(x_2, n_2)$  as in (39), the desired exponential estimate containing  $e^{\text{const}\cdot u}$  for the single integral is obtained along the lines of Lemma 6.2 in Borodin and Ferrari (2008). This completes the proof.  $\square$

LEMMA 4.17. *Assume that now both the points  $(x_j, n_j)$  ( $j = 1, 2$ ) are at the lower left edge or in the corresponding facet as in (39). Let  $|\tilde{w}_1 - \tilde{w}_2|$  be bounded away from zero uniformly in  $N$ . Then*

$$\begin{aligned} & |K(x_1, n_1; x_2, n_2)| \\ & \leq \frac{C e^{N(\mathfrak{M}\tilde{S}_1(\tilde{w}_1) - \mathfrak{M}\tilde{S}_2(\tilde{w}_2))}}{N^{2/3}} \\ & \quad \times \exp\left\{-C_1 N^{2/3}\left(\eta_{\text{fb}}\left(\frac{x_1}{N}\right) - \frac{n_1}{N}\right) - C_2 N^{2/3}\left(\eta_{\text{fb}}\left(\frac{x_2}{N}\right) - \frac{n_2}{N}\right)\right\} \end{aligned}$$

uniformly in  $N$ , where  $C, C_1, C_2 > 0$ .

PROOF. This lemma is obtained similarly to the previous Lemma 4.16, but now we derive exponential estimates for both  $w$  and  $z$  integrals.  $\square$

**5. Completing the proofs.** In this section we finish the proof of Theorem 1.2 (Sections 5.1–5.3), and then explain how it leads to Theorem 1.3 (Section 5.4).

5.1. *Expanding determinants in s-fold sums (21).* Fix pairwise distinct points  $(\chi_1, \eta_1), \dots, (\chi_s, \eta_s)$  inside the liquid region  $\mathcal{D}$ . In Section 3 we showed that the expectation  $\mathbb{E}(H_N(\chi_1, \eta_1) \cdots H_N(\chi_s, \eta_s))$  of Theorem 1.2 can be expressed as a linear combination of expressions like (21)

$$(41) \quad \sum_{y_1=x_1+1}^{x'_1} \cdots \sum_{y_r=x_r+1}^{x'_r} \sum_{m_{r+1}=n_{r+1}+1}^{n'_{r+1}} \cdots \sum_{m_s=n_s+1}^{n'_s} \det \begin{bmatrix} A_{1,1} & A_{1,2} \\ A_{2,1} & A_{2,2} \end{bmatrix},$$

where the matrix blocks are given in (22). Each such  $s$ -fold sum corresponds to a choice of one linear (horizontal or vertical) part on every  $i$ th path starting at the point  $(\chi_i, \eta_i)$ ,  $i = 1, \dots, s$ ; see Figure 10. Throughout the section we assume that these paths on Figure 10 along which we calculate the height function are separated from tangent points as explained in the proof of Lemma 4.15.

Let us consider one  $s$ -fold sum as in (41). Expanding the above  $s \times s$  determinant, we write it as the sum over permutations  $\sigma \in \mathfrak{S}(s)$  of terms each of which is  $\text{sgn } \sigma$  times the product of matrix elements with indices  $(i, \sigma_i)$ ,  $i = 1, \dots, s$ . Express  $\sigma$  as a union of several disjoint cycles. Since the matrix  $\begin{bmatrix} A_{1,1} & A_{1,2} \\ A_{2,1} & A_{2,2} \end{bmatrix}$  has zero diagonal entries, all these cycles must have length  $\geq 2$ . In the next subsection we will show that the contribution of permutations containing cycles of length  $\geq 3$  becomes negligible in the limit as  $N \rightarrow \infty$ .

5.2. *Contribution of permutations with cycles of length  $\geq 3$ .* Let the permutation  $\sigma \in \mathfrak{S}(s)$  contain a cycle of length  $\ell \geq 3$ . To shorten the notation, we assume that this cycle is  $1 \rightarrow 2 \rightarrow \dots \rightarrow \ell \rightarrow 1$ . In the expansion of the determinant in (41) we take the product of the kernels and do a horizontal (over

$y_j = x_j + 1, \dots, x'_j$ ) or vertical (over  $m_j = n_j + 1, \dots, n'_j$ ) summation. Let us collect terms corresponding to a fixed index  $i = 1, \dots, \ell$ . We will assume that the shifts  $i \pm 1$  are given mod  $\ell$ . There are four possible cases we consider:

(V) The summation related to the index  $i$  is performed over a vertical segment:  $\{(x_i, m_i) : m_i = n_i + 1, \dots, n'_i\}$ . It can happen that this vertical segment crosses the lower left frozen boundary; see Figure 10. Thus, we split the summation into three parts according to (37)–(39).

(V; edge or facet) Summation over  $I_1 := \{n_i + 1, \dots, n'_i\} \cap \{m_i : m_i \leq N\eta_{\text{fb}}(x_i/N) + cN^{1/3}\}$ . Here  $\eta_{\text{fb}}$  is defined in Section 4.6. We need to consider

$$(42) \quad - \sum_{m_i \in I_1} K(t_{i-1}, u_{i-1}; x_i + 1, m_i - 1) K(x_i, m_i; t_{i+1}, u_{i+1}).$$

The minus sign is coming from the second factor; see (22). Here and below, the points  $(t_{i\pm 1}, u_{i\pm 1})$  (corresponding to indices  $\sigma_i$  and  $\sigma_i^{-1}$ ) are equal to  $(y_j, n_j)$  or  $(x_j + 1, m_j - 1)$  for suitable  $j$ ; see (22).

LEMMA 5.1. *The contribution of the sum (42) over  $I_1$  goes to zero as  $N \rightarrow \infty$ .*

PROOF. By Lemmas 4.16 and 4.17, we can write

$$\begin{aligned} & \left| \sum_{m_i \in I_1} K(t_{i-1}, u_{i-1}; x_i + 1, m_i - 1) K(x_i, m_i; t_{i+1}, u_{i+1}) \right| \\ & \leq \frac{\text{const}}{N^{2/3}} \sum_{m_i \in I_1} \exp\left\{-\text{const} \cdot N^{2/3} \left(\eta_{\text{fb}}\left(\frac{x_i}{N}\right) - \frac{m_i}{N}\right)\right\} \times \text{terms in } (t_{i\pm 1}, u_{i\pm 1}) \\ & \leq \frac{\text{const}}{N^{1/3}} \times \text{terms in } (t_{i\pm 1}, u_{i\pm 1}). \end{aligned}$$

To get the first estimate above we employ considerations similar to Corollary 4.12; this may change the bound only by a factor of a constant. The second estimate completes the proof.  $\square$

(V; close to edge) Summation over  $I_2 := \{n_i + 1, \dots, n'_i\} \cap \{m_i : cN^{1/3} + N\eta_{\text{fb}}(x_i/N) \leq m_i \leq N^{2/3} + N\eta_{\text{fb}}(x_i/N)\}$ .

LEMMA 5.2. *The contribution of the sum (42), where  $m_i$  runs over  $I_2$  instead of  $I_1$ , also goes to zero as  $N \rightarrow \infty$ .*

PROOF. We have

$$\begin{aligned} & \left| \sum_{m_i \in I_2} K(t_{i-1}, u_{i-1}; x_i + 1, m_i - 1) K(x_i, m_i; t_{i+1}, u_{i+1}) \right| \\ & \leq \frac{\text{const}}{N} \sum_{m_i \in I_2} \frac{1}{|S''_i(\mathbf{w}(i))|} \times \text{terms in } (t_{i\pm 1}, u_{i\pm 1}). \end{aligned}$$

Here we have used a shorthand notation  $w(i) := w(\frac{x_i}{N}, \frac{m_i}{N})$ , and the same for  $S_i$ ; see also (26). Also, as in the previous lemma we use argument similar to Corollary 8, but this again may only change the constant in the bound.

Let us bound  $|S_i''(w(i))|$  from below. Observe that the third derivative  $S'''(w)$  is bounded away from zero for small  $\Im w$ , if  $\Re w$  belongs to a bounded interval to the left of the point  $a_1 \in \mathbb{R}$  from (1). Indeed, under the map  $w^{-1} : \mathbb{H} \rightarrow \mathcal{D}$ , such  $w$ 's are close to the lower left edge and are separated from the tangent points. Thus, we can write  $|S_i''(w(i))| \geq \text{const} \cdot \Im w(i)$ .

Next, it can be seen that the imaginary part  $\Im w(i)$  can be bounded from below by  $\text{const} \cdot |w_\eta(\chi, \eta) \cdot |\frac{m_i}{N} - \eta_{\text{fb}}(\frac{x_i}{N}) + O(N^{-1/6})|$ , where  $(\chi, \eta) \in \mathcal{D}$  is some intermediate point closer to the edge than  $(\frac{x_i}{N}, \frac{m_i}{N})$ . Instead of  $O(N^{-1/6})$  one could take any correction term which is asymptotically smaller than  $\frac{m_i}{N} - \eta_{\text{fb}}(\frac{x_i}{N})$ . We have [see also Petrov (2012), Section 7.6]

$$w_\eta = \frac{w - \chi}{\eta - 1 + (w - \chi)(w - \chi + 1 - \eta)\Sigma(w)},$$

where

$$\Sigma(w) = \sum_{i=1}^k \left( \frac{1}{w - b_i} - \frac{1}{w - a_i} \right).$$

Using the formula for the action (25), we see that

$$(43) \quad w_\eta = -\frac{1}{S''(w(\chi, \eta); \chi, \eta) \cdot (w - \chi + 1 - \eta)}.$$

Therefore,

$$\begin{aligned} |S_i''(w(i))| &\geq \text{const} \cdot \left| \frac{m_i/N - \eta_{\text{fb}}(x_i/N) + O(N^{-1/6})}{S''(w(\chi, \eta); \chi, \eta)} \right| \\ &\geq \text{const} \cdot N^{1/3} \left| \frac{m_i}{N} - \eta_{\text{fb}}\left(\frac{x_i}{N}\right) + O(N^{-1/6}) \right| \end{aligned}$$

[we estimate the second derivative in the denominator using (38)]. We obtain

$$\begin{aligned} \frac{\text{const}}{N} \sum_{m_i \in I_2} \frac{1}{|S_i''(w(i))|} &\leq \sum_{m_i \in I_2} \frac{\text{const} \cdot N^{-1/3}}{|m_i - N\eta_{\text{fb}}(x_i/N) + O(N^{5/6})|} \\ &\leq \text{const} \cdot N^{-1/3} \ln N. \end{aligned}$$

This completes the proof.  $\square$

It is not hard to see from Lemmas 5.1 and 5.2 that in the two remaining cases (V; bulk) and (H) (see below) we may assume that all the  $\ell$  variables we are summing over (which correspond to vertical and horizontal summations) always belong to the bulk of the system in the sense of (37).

(V; bulk) Summation over  $I_3 := \{n_i + 1, \dots, n'_i\} \cap \{m_i : m_i \geq N^{2/3} + N\eta_{\text{fb}}(x_i/N)\}$ . From what was said right above, we may as well take  $I_3 = \{n_i + 1, \dots, n'_i\}$ . We will investigate the asymptotics of (42) where now  $m_i$  runs over  $I_3$  instead of  $I_1$ .

Similarly to the proof of Lemma 5.2, let us denote  $w(i) = w(\frac{x_i}{N}, \frac{m_i}{N})$ ,  $w(i \pm 1) := w(\frac{t_{i\pm 1}}{N}, \frac{u_{i\pm 1}}{N})$ , and same for  $S_i, \Xi_i$  [see also (26)]. Also, let  $\beta_z(i)$  denote the argument of the tangent vector to the  $z$  contour at the point  $w(i)$  as on Figure 11, and analogously for  $\beta_w(i)$ . It can be readily checked [using the global structure of the  $z$  and  $w$  contours (Section 4.3)] that

$$(44) \quad \begin{aligned} \beta_z(i) &= \beta_w(i) + \frac{\pi}{2} \quad \text{and} \\ \beta_z(i) + \beta_w(i) + \arg S_i''(w(i)) &= \frac{3\pi}{2} + 2\pi q \quad (\text{for some } q \in \mathbb{Z}). \end{aligned}$$

By the nature of our paths (on Figure 10), the points  $(t_{i\pm 1}, u_{i\pm 1})$  are sufficiently far from  $(x_i, m_i)$ . Thus we may use Proposition 4.11 and Corollary 4.12 and write (here and below  $\delta > 0$  is sufficiently small and fixed)

$$(45) \quad \begin{aligned} & - \sum_{m_i \in I_3} K(t_{i-1}, u_{i-1}; x_i + 1, m_i - 1) K(x_i, m_i; t_{i+1}, u_{i+1}) \\ &= - \frac{1 + O(N^{-\delta/2})}{2\pi N} \\ & \quad \times \sum_{m_i \in I_3} \frac{1}{|S_i''(w(i))|} \\ & \quad \times \left\{ \left[ \frac{e^{i\beta_z(i)}}{w(i-1) - w(i)} \cdot \frac{e^{i\beta_w(i)}}{w(i) - w(i+1)} \frac{1}{\Xi_i(w(i))} \frac{w(i) - x_i/N}{1 - m_i/N} \right. \right. \\ & \quad - \frac{e^{i\beta_z(i)}}{w(i-1) - w(i)} \cdot \frac{e^{-i\beta_w(i)}}{\bar{w}(i) - w(i+1)} \frac{e^{-2Ni \cdot \Im S_i(w(i))}}{|\Xi_i(w(i))|} \\ & \quad \times \frac{w(i) - x_i/N}{1 - m_i/N} - \frac{e^{-i\beta_z(i)}}{w(i-1) - \bar{w}(i)} \cdot \frac{e^{i\beta_w(i)}}{w(i) - w(i+1)} \\ & \quad \times \frac{e^{2Ni \cdot \Im S_i(w(i))}}{|\Xi_i(w(i))|} \frac{\bar{w}(i) - x_i/N}{1 - m_i/N} + \frac{e^{-i\beta_z(i)}}{w(i-1) - \bar{w}(i)} \\ & \quad \left. \left. \times \frac{e^{-i\beta_w(i)}}{\bar{w}(i) - w(i+1)} \frac{1}{\Xi_i(\bar{w}(i))} \frac{\bar{w}(i) - x_i/N}{1 - m_i/N} \right] \right. \\ & \quad \left. \times (\text{terms in } (t_{i\pm 1}, u_{i\pm 1})) + \circ \right\}. \end{aligned}$$

Here and below  $\circlearrowleft$  denotes all additional terms (there are 12 of them in the above formula) which are obtained by replacing  $w(i - 1)$  and/or  $w(i + 1)$  by the corresponding complex conjugate points.

Arguing analogously to Section 5.3 in [Borodin and Ferrari \(2008\)](#) [case (a/3)], one can show that the contribution of the oscillating terms above containing  $e^{\pm 2Ni \Im S_i(w(i))}$  becomes negligible [of order  $O(N^{-1/3+\varepsilon})$ ] in the limit. The remaining terms are smooth and change over distances  $m_i \sim N$ . Therefore, up to an error of order  $O(N^{-1/3})$ , we can replace the summation over  $m_i$  in (45) by integration in the scaled variables. Namely, setting  $\mu := m_i/N$ ,  $\eta := (n_i + 1)/N$ ,  $\eta' := n'_i/N$ ,  $\chi := x_i/N$ , we can rewrite (45) as

$$(46) \quad -\frac{1 + O(N^{-\delta/2})}{2\pi} \int_{\eta}^{\eta'} d\mu \frac{1}{|S_i''(w(i))|} \\ \times \left\{ \left[ \frac{e^{i\beta_z(i)}}{w(i-1) - w(i)} \cdot \frac{e^{i\beta_w(i)}}{w(i) - w(i+1)} \frac{1}{\Xi_i(w(i))} \frac{w(i) - \chi}{1 - \mu} \right. \right. \\ \left. \left. + \frac{e^{-i\beta_z(i)}}{w(i-1) - \bar{w}(i)} \cdot \frac{e^{-i\beta_w(i)}}{\bar{w}(i) - w(i+1)} \frac{1}{\Xi_i(\bar{w}(i))} \frac{\bar{w}(i) - \chi}{1 - \mu} \right] \right. \\ \left. \times (\text{terms in } (t_{i\pm 1}, u_{i\pm 1})) + \circlearrowleft \right\}.$$

The next step we perform is a change of variables. For the term with  $w(i)$ , we set  $\zeta_i^+ := w(i) = w(\chi, \mu)$ . The integration path  $\Gamma_i^+$  for  $\zeta_i^+$  is from  $w(\chi, \eta)$  to  $w(\chi, \eta')$ , that is,  $\Gamma_i^+$  is the image of the vertical line from  $\eta$  to  $\eta'$  in  $\mathcal{D}$  under the map  $w: \mathcal{D} \rightarrow \mathbb{H}$ . Form the results of [Petrov \(2012\)](#), we have [see also (43)]

$$\frac{\partial \zeta_i^+}{\partial \mu} = -\frac{1}{S_i''(w(i)) \cdot \Xi_i(w(i))} \frac{w(i) - \chi}{1 - \mu}.$$

Symmetrically, for the term with  $\bar{w}(i)$ , let  $\zeta_i^- := \bar{w}(i) = \bar{w}(\chi, \mu)$ , and the integration path  $\Gamma_i^-$  for  $\zeta_i^-$  is conjugate to that for  $\zeta_i^+$ . It can be readily verified [in particular, using (44)] that the above integral (46) can be rewritten as the sum of two integrals,

$$(47) \quad \frac{1}{2\pi i} \sum_{\varepsilon_i = \pm} \varepsilon_i \int_{\Gamma_i^{\varepsilon_i}} d\zeta_i^{\varepsilon_i} \left[ \frac{1}{w(i-1) - \zeta_i^{\varepsilon_i}} \frac{1}{\zeta_i^{\varepsilon_i} - w(i+1)} \right. \\ \left. \times \text{terms in } (t_{i\pm 1}, u_{i\pm 1}) + \circlearrowleft \right].$$

There is an additional minus sign for  $\Gamma_i^-$  because of a different phase  $-(\beta_z(i) + \beta_w(i))$  in the second summand in (46). Thus we have established the following fact:

PROPOSITION 5.3. *The sum (42), where  $m_i$  runs over  $I_3$  instead of  $I_1$ , is [up to a factor of  $1 + O(N^{-\delta/2})$ , where  $\delta > 0$  is a fixed sufficiently small constant] equal to the sum of two integrals (47).*

(H) The summation related to the index  $i$  is performed over a horizontal segment,  $\{(y_i, n_i) : y_i = x_i + 1, \dots, x'_i\}$ .

PROPOSITION 5.4. *The horizontal sum has the following asymptotics:*

$$\begin{aligned} & \sum_{y_i=x_i+1}^{x'_i} K(t_{i-1}, u_{i-1}; y_i, n_i) K(y_i, n_i; t_{i+1}, u_{i+1}) \\ &= \frac{1 + O(N^{-\delta/2})}{2\pi i} \\ & \quad \times \sum_{\varepsilon_i=\pm} \varepsilon_i \int_{\Gamma_i^{\varepsilon_i}} d\zeta_i^{\varepsilon_i} \left[ \frac{1}{w(i-1) - \zeta_i^{\varepsilon_i}} \frac{1}{\zeta_i^{\varepsilon_i} - w(i+1)} \right. \\ & \quad \left. \times \text{terms in } (t_{i\pm 1}, u_{i\pm 1}) + \bigcirc \right], \end{aligned}$$

where all the notation is as in the previous case, except that now the path of integration  $\Gamma_i^+$  connects  $w(\frac{x_i+1}{N}, \frac{n_i}{N})$  and  $w(\frac{x'_i}{N}, \frac{n_i}{N})$ , and  $\Gamma_i^-$  is the conjugate of  $\Gamma_i^+$ .

PROOF. This is established in the same way as Proposition 5.3.  $\square$

After considering the four above cases, we conclude this subsection with the desired statement about permutations  $\sigma \in \mathfrak{S}(\mathfrak{s})$  having cycles of length  $\ell \geq 3$ :

PROPOSITION 5.5. *Consider one  $\mathfrak{s}$ -fold sum (41) and expand the  $\mathfrak{s} \times \mathfrak{s}$  determinant as a sum over permutations  $\sigma \in \mathfrak{S}(\mathfrak{s})$ . Then the contribution of those  $\sigma$ 's having cycles of length  $\ell \geq 3$  goes to zero as  $N \rightarrow \infty$ .*

PROOF. From Lemmas 5.1, 5.2 and Propositions 5.3, 5.4 it follows that each cycle  $j_1 \rightarrow j_2 \rightarrow \dots \rightarrow j_\ell \rightarrow j_1$  in  $\sigma$  asymptotically produces the following sum of  $\ell$ -fold integrals:

$$\frac{1}{(2\pi i)^\ell} \sum_{\varepsilon_1, \dots, \varepsilon_\ell = \pm} \varepsilon_1 \cdots \varepsilon_\ell \int_{\Gamma_1^{\varepsilon_1}} d\zeta_1^{\varepsilon_1} \cdots \int_{\Gamma_\ell^{\varepsilon_\ell}} d\zeta_\ell^{\varepsilon_\ell} \prod_{i=1}^{\ell} \frac{1}{z_{j_i}^{\varepsilon_{j_i}} - z_{j_{i+1}}^{\varepsilon_{j_{i+1}}}}.$$

On the other hand, by Kenyon (2008), Lemma 7.3, we have

$$\sum_{\text{all } \ell\text{-cycles } \tau \in \mathfrak{S}(\ell)} \prod_{i=1}^{\ell} \frac{1}{U_{\tau_i} - U_{\tau_{i+1}}} = 0, \quad \ell \geq 3.$$

This concludes the proof.  $\square$

5.3. *Contribution of fixed-point-free involutions.* In Sections 5.1–5.2 we have shown that if one expands the determinant in (41) as a sum over permutations  $\sigma \in \mathfrak{S}(\mathfrak{s})$ , then the contribution of permutations  $\sigma$  which are not fixed-point-free involutions (= pairings) becomes negligible in the limit. Collecting all summands of the form (41) corresponding to the expectation  $\mathbb{E}(H_N(\chi_1, \eta_1) \cdots H_N(\chi_{\mathfrak{s}}, \eta_{\mathfrak{s}}))$  [with pairwise distinct positions  $(\chi_1, \eta_1), \dots, (\chi_{\mathfrak{s}}, \eta_{\mathfrak{s}})$ ], we see that

$$\begin{aligned} & \mathbb{E}(H_N(\chi_1, \eta_1) \cdots H_N(\chi_{\mathfrak{s}}, \eta_{\mathfrak{s}})) \\ &= (1 + O(N^{-\delta/2})) \\ & \times \sum_{\text{pairings } \sigma \in \mathfrak{S}(\mathfrak{s})} \prod_{i=1}^{s/2} \frac{1}{(2\pi i)^2} \\ & \quad \times \int_{\bar{w}(\chi_{\sigma(2i-1)}, \eta_{\sigma(2i-1)})}^{w(\chi_{\sigma(2i-1)}, \eta_{\sigma(2i-1)})} d\zeta_{2i-1} \int_{\bar{w}(\chi_{\sigma(2i)}, \eta_{\sigma(2i)})}^{w(\chi_{\sigma(2i)}, \eta_{\sigma(2i)})} d\zeta_{2i} \\ & \quad \times \frac{1}{(\zeta_{2i-1} - \zeta_{2i})^2}. \end{aligned}$$

Note the additional minus sign coming from the signature of each transposition. The paths of integration in  $\mathbb{H}$  from  $\bar{w}(\chi_{\sigma(j)}, \eta_{\sigma(j)})$  to  $w(\chi_{\sigma(j)}, \eta_{\sigma(j)})$  are obtained by linearity (Section 3.2) and by symmetry of the contours  $\Gamma_j^{\pm}$  in Propositions 5.3, 5.4.

Each integral above can be explicitly evaluated,

$$\begin{aligned} & \frac{1}{(2\pi i)^2} \int_{\bar{w}_1}^{w_1} d\zeta_1 \int_{\bar{w}_2}^{w_2} d\zeta_2 \frac{1}{(\zeta_1 - \zeta_2)^2} \\ &= -\frac{1}{4\pi^2} \ln \left( \frac{(w_1 - w_2)(\bar{w}_1 - \bar{w}_2)}{(w_1 - \bar{w}_2)(\bar{w}_1 - w_2)} \right) = \frac{\mathcal{G}(w_1, w_2)}{\pi}, \end{aligned}$$

where  $\mathcal{G}$  is the Green function (5). With this step we have completed the proof of Theorem 1.2.

5.4. *Convergence to GFF: Proof of Theorem 1.3.* Our aim now is to prove the weak convergence of  $\sqrt{\pi} H_N(\chi, \eta)$  (viewed as a generalized function on  $\mathcal{D}$ ) to the  $w$ -pullback of the Gaussian free field GFF on  $\mathbb{H}$ ; see Sections 1.6–1.7. In order to do that, we need an additional estimate:

LEMMA 5.6. *For any  $\varepsilon > 0$  and any  $\mathfrak{s}$  points  $(\chi_1, \eta_1), \dots, (\chi_{\mathfrak{s}}, \eta_{\mathfrak{s}}) \in \mathcal{D}$  (not necessarily pairwise distinct) we have the bound*

$$\mathbb{E}(H_N(\chi_1, \eta_1) \cdots H_N(\chi_{\mathfrak{s}}, \eta_{\mathfrak{s}})) = O(N^\varepsilon), \quad N \rightarrow \infty.$$

PROOF. If all the points are distinct, we have a better bound  $O(1)$  by Theorem 1.2. Next, assume that, say,  $(\chi_1, \eta_1) = (\chi_2, \eta_2)$ . Connect  $(\chi_1, \eta_1)$  with the



lower left edge by two paths which are close to each other only in a neighborhood of  $(\chi_1, \eta_1)$ . As explained in Section 3, we calculate  $(H_N(\chi_1, \eta_1))^2$  as a product of sums over these two paths. Fix small  $\delta > 0$ , and in each sum consider separately the  $N^{1/2+\delta}$  terms corresponding to  $N^{-1/2+\delta}$ -neighborhood of  $(\chi_1, \eta_1)$ . All other terms give a contribution of order  $O(1)$  because they involve points which are far apart, and so one can argue similarly to Proposition 4.11 and Theorem 1.2. On the other hand, the terms corresponding to close points are estimated using Proposition 4.10 and Lemma 4.13. The former gives growth of order  $O(\ln N)^2$  coming from the single integral in the correlation kernel (30), and the latter provides a bound  $O(N^{2\delta})$  which comes from the double integral in (30). This completes the proof. See also the end of Section 7 in Kenyon (2008).  $\square$

Now we finish the proof of Theorem 1.3. We argue similarly to Borodin and Ferrari (2008), Section 5.5. It suffices to establish that [see (9)]

$$(48) \quad \begin{aligned} & \lim_{N \rightarrow \infty} \pi^{s/2} \mathbb{E} \left( \prod_{i=1}^s \int_{\mathcal{D}} \phi_i(\chi_i, \eta_i) H_N(\chi_i, \eta_i) d\chi_i d\eta_i \right) \\ &= \mathbb{E} \left( \prod_{i=1}^s \int_{\mathbb{H}} \phi_i(\mathbf{w}^{-1}(z_i)) J(z_i) \text{GFF}(z_i) |dz_i|^2 \right), \end{aligned}$$

where  $\phi_1, \dots, \phi_s$  are smooth compactly supported test functions on  $\mathcal{D}$ . This convergence of moments implies the weak convergence (9) of  $\sqrt{\pi} \int_{\mathcal{D}} \phi(\chi, \eta) \times H_N(\chi, \eta) d\chi d\eta$  to the corresponding Gaussian random variable  $\int_{\mathbb{H}} \phi(\mathbf{w}^{-1}(z)) \times J(z) \text{GFF}(z) |dz|^2$ , as well as an obvious multidimensional analogue of this fact involving convergence to a Gaussian vector.

The left-hand side of (48) is equal to

$$\int_{\mathbb{H}^s} \prod_{i=1}^s |dz_i|^2 (\phi_i(\mathbf{w}^{-1}(z_i)) J(z_i)) \mathbb{E}(H_N(\mathbf{w}^{-1}(z_1)) \cdots H_N(\mathbf{w}^{-1}(z_s))).$$

We split this integration over  $\mathbb{H}^s$  into two parts, one where the points  $z_j$  are sufficiently far apart,

$$\mathbb{H}_\delta^s := \{(z_1, \dots, z_s) \in \mathbb{H}^s : |z_i - z_j| \geq N^{-1/2+\delta}, 1 \leq i < j \leq s\},$$

and the remaining part  $\mathbb{H}^s \setminus \mathbb{H}_\delta^s$  where some of them are close. As usual,  $\delta > 0$  is small and fixed.

For the integration over  $\mathbb{H}_\delta^s$  we use Propositions 5.3 and 5.4 to write

$$\begin{aligned} & \int_{\mathbb{H}_\delta^s} \prod_{i=1}^s |dz_i|^2 (\phi_i(\mathbf{w}^{-1}(z_i)) J(z_i)) \mathbb{E}(H_N(\mathbf{w}^{-1}(z_1)) \cdots H_N(\mathbf{w}^{-1}(z_s))) \\ &= \int_{\mathbb{H}_\delta^s} \prod_{i=1}^s |dz_i|^2 (\phi_i(\mathbf{w}^{-1}(z_i)) J(z_i)) \mathbb{E}(\text{GFF}(z_1) \cdots \text{GFF}(z_s)) + O(N^{-\delta/2}). \end{aligned}$$

Since the logarithms in  $\mathbb{E}(\text{GFF}(z_1) \cdots \text{GFF}(z_s))$  (see Section 1.6) are integrable around zero, we may replace the above integral over  $\mathbb{H}_\delta^{\mathbb{S}}$  by the same integral over  $\mathbb{H}^{\mathbb{S}}$ .

The integral over the complement  $\mathbb{H}^{\mathbb{S}} \setminus \mathbb{H}_\delta^{\mathbb{S}}$  is bounded using Lemma 5.6,

$$\left| \int_{\mathbb{H}^{\mathbb{S}} \setminus \mathbb{H}_\delta^{\mathbb{S}}} \prod_{i=1}^s |dz_i|^2 (\phi_i(w^{-1}(z_i)) J(z_i)) \mathbb{E}(H_N(w^{-1}(z_1)) \cdots H_N(w^{-1}(z_s))) \right| \leq \text{const} \cdot (N^{-1/2+\delta})^2 N^\varepsilon,$$

where the constant depends only on our test functions  $\phi_j$ . This last estimate implies the desired convergence (48), and completes the proof of Theorem 1.3.

**Acknowledgments.** I would like to thank Alexei Borodin for interest in my work and many fruitful discussions, and Vadim Gorin, Alexey Bufetov and Jeffrey Kuan for useful comments.

## REFERENCES

- BAIK, J., KRIECHERBAUER, T., MCLAUGHLIN, K. T. R. and MILLER, P. D. (2007). *Discrete Orthogonal Polynomials: Asymptotics and Applications*. *Annals of Mathematics Studies* **164**. Princeton Univ. Press, Princeton, NJ. [MR2283089](#)
- BORODIN, A. (2011). Determinantal point processes. In *Oxford Handbook of Random Matrix Theory* (G. Akemann, J. Baik and P. Di Francesco, eds.). Oxford Univ. Press, Oxford.
- BORODIN, A. and FERRARI, P. L. (2008). Anisotropic growth of random surfaces in  $2 + 1$  dimensions. Available at [arXiv:0804.3035](#) [math-ph].
- BORODIN, A., FERRARI, P. L. and SASAMOTO, T. (2008). Large time asymptotics of growth models on space-like paths. II. PNG and parallel TASEP. *Comm. Math. Phys.* **283** 417–449. [MR2430639](#)
- BORODIN, A. and GORIN, V. (2009). Shuffling algorithm for boxed plane partitions. *Adv. Math.* **220** 1739–1770. [MR2493180](#)
- BORODIN, A., GORIN, V. and RAINS, E. M. (2010).  $q$ -distributions on boxed plane partitions. *Selecta Math. (N.S.)* **16** 731–789. [MR2734330](#)
- BORODIN, A., OKOUNKOV, A. and OLSHANSKI, G. (2000). Asymptotics of Plancherel measures for symmetric groups. *J. Amer. Math. Soc.* **13** 481–515 (electronic). [MR1758751](#)
- COHN, H., KENYON, R. and PROPP, J. (2001). A variational principle for domino tilings. *J. Amer. Math. Soc.* **14** 297–346 (electronic). [MR1815214](#)
- COHN, H., LARSEN, M. and PROPP, J. (1998). The shape of a typical boxed plane partition. *New York J. Math.* **4** 137–165 (electronic). [MR1641839](#)
- DESTAINVILLE, N. (1998). Entropy and boundary conditions in random rhombus tilings. *J. Phys. A* **31** 6123–6139. [MR1637731](#)
- DESTAINVILLE, N., MOSSERI, R. and BAILLY, F. (1997). Configurational entropy of codimension-one tilings and directed membranes. *J. Stat. Phys.* **87** 697–754. [MR1459040](#)
- DUITS, M. (2011). The Gaussian free field in an interlacing particle system with two jump rates. Available at [arXiv:1105.4656](#) [math-ph].
- GORIN, V. E. (2008). Nonintersecting paths and the Hahn orthogonal polynomial ensemble. *Funct. Anal. Appl.* **42** 180–197.
- HOUGH, J. B., KRISHNAPUR, M., PERES, Y. and VIRÁG, B. (2006). Determinantal processes and independence. *Probab. Surv.* **3** 206–229. [MR2216966](#)

- KENYON, R. (2008). Height fluctuations in the honeycomb dimer model. *Comm. Math. Phys.* **281** 675–709. [MR2415464](#)
- KENYON, R. (2009). Lectures on dimers. In *Statistical Mechanics. IAS/Park City Math. Ser.* **16** 191–230. Amer. Math. Soc., Providence, RI. [MR2523460](#)
- KENYON, R. and OKOUNKOV, A. (2007). Limit shapes and the complex Burgers equation. *Acta Math.* **199** 263–302. [MR2358053](#)
- KENYON, R., OKOUNKOV, A. and SHEFFIELD, S. (2006). Dimers and amoebae. *Ann. of Math. (2)* **163** 1019–1056. [MR2215138](#)
- KUAN, J. (2011). The Gaussian free field in interlacing particle systems. Available at [arXiv:1109.4444](#) [math-ph].
- OKOUNKOV, A. (2002). Symmetric functions and random partitions. In *Symmetric Functions 2001: Surveys of Developments and Perspectives* (S. Fomin, ed.). Kluwer Academic, Dordrecht.
- OKOUNKOV, A. and RESHETIKHIN, N. (2003). Correlation function of Schur process with application to local geometry of a random 3-dimensional Young diagram. *J. Amer. Math. Soc.* **16** 581–603 (electronic). [MR1969205](#)
- PETROV, L. (2012). Asymptotics of random lozenge tilings via Gelfand–Tsetlin schemes. Available at [arXiv:1202.3901](#) [math.PR].
- SHEFFIELD, S. (2005). Random surfaces. *Astérisque* **304** vi+175. [MR2251117](#)
- SHEFFIELD, S. (2007). Gaussian free fields for mathematicians. *Probab. Theory Related Fields* **139** 521–541. [MR2322706](#)
- SOSHNIKOV, A. (2000). Determinantal random point fields. *Russian Math. Surveys* **55** 923–975.

DEPARTMENT OF MATHEMATICS  
 NORTHEASTERN UNIVERSITY  
 360 HUNTINGTON AVE.  
 BOSTON, MASSACHUSETTS 02115  
 USA  
 AND  
 INSTITUTE FOR INFORMATION  
 TRANSMISSION PROBLEMS  
 BOLSHOY KARETNY PER. 19  
 MOSCOW, 127994  
 RUSSIA  
 E-MAIL: [l.petrov@neu.edu](mailto:l.petrov@neu.edu)